IEEE Access
Multidisciplinary ⋮ Rapid Review ⋮ Open Access Journal

Received 19 March 2026, accepted 23 April 2026, date of publication 6 May 2026, date of current version 13 May 2026.

Digital Object Identifier 10.1109/ACCESS.2026.3690305

RESEARCH ARTICLE

On OFDM Ranging Performance Degradation in Multipath Scenarios: Bias and Misspecified Cramér–Rao Bounds

LUCAS ALVAREZ NAVARRO[1], CHRISTIAN C. J. M. TIBERIUS[1], AND GERARD J. M. JANSSEN[2]
[1]Department of Geoscience and Remote Sensing, Delft University of Technology, 2628 CN Delft, The Netherlands
[2]Signal Processing Systems Group, Delft University of Technology, 2628 CD Delft, The Netherlands

Corresponding author: Lucas Alvarez Navarro (lalvareznavarr@tudelft.nl)

This work was supported in part by Dutch Research Council (NWO) through the Project SuperGPS-2 under Grant 19783, and in part by Delft University of Technology (TU Delft) Library through the Open Access Fund.

ABSTRACT Multipath propagation represents a dominant error source limiting the accuracy of radio-based ranging and positioning in urban environments. Conventional ranging estimators typically estimate only the range of the first arriving path while neglecting the multipath components. This introduces a bias and causes the estimator's variance to diverge from the Cramér-Rao Bound (CRB). While extensive research has established performance bounds for estimators that jointly estimate all paths, the specific impact on the variance of ignoring these components remains largely unexplored. This paper derives bounds on the bias, variance, and mean square error (MSE) for ranging in multipath channels for the purpose of positioning. We consider Orthogonal Frequency Division Multiplexing (OFDM) signals in multipath channels with deterministic path delays and gains. The paper focuses on time-delay estimation (TDE) in the mid-to-high signal-to-noise ratio (SNR) regime under two scenarios: (i) when the receiver jointly estimates all propagation paths, and (ii) when the receiver underestimates the number of paths. Specifically, for the latter case, we derive a semi closed-form expression for the variance of the time-delay estimator that considers a single-path when in reality there are L paths. This derivation is based on the misspecified Cramér-Rao bound (MCRB). Although unmodelled multipath has been traditionally viewed as detrimental to time-delay estimation, we reveal that in some cases the estimation variance improves. For a two-path channel we show that the variance depends on the relative gain, carrier phase, and separation of the paths. Additionally, the estimation bias is upper-bounded by constructive and destructive path interference. Finally, we empirically process a six-path simulated channel frequency response with fixed path delays and gains, to demonstrate that the derived MSE bound is tight for mid-to-high SNRs. This work characterizes the impact of multipath propagation on the variance of time-delay estimation, which is essential for designing accurate ranging signals and estimators in urban scenarios.

INDEX TERMS Time-delay estimation (TDE), positioning, OFDM, multipath, bias, performance bounds, misspecified Cramér-Rao bound (MCRB).

I. INTRODUCTION

Current Position, Navigation, and Timing (PNT) services heavily rely on Global Navigation Satellite Systems (GNSS). However, GNSS are vulnerable to malicious interference like jamming and spoofing, and its accuracy degrades in dense urban scenarios due to signal blockage and multipath propagation. Terrestrial wireless networks, such as the fifth generation (5G) communication system, present a promising solution by supporting ranging capabilities, but their accuracy is limited by the narrow bandwidth allocated for ranging purposes. While next-generation systems provide larger bandwidths for ranging, they remain susceptible to multipath propagation. Therefore, characterizing its impact

The associate editor coordinating the review of this manuscript and approving it for publication was Chuan Heng Foh.

is essential to design robust signals and resilient estimation algorithms.

Wireless communication systems often employ Orthogonal Frequency Division Multiplexing (OFDM). In these systems, most of the time and frequency resources are allocated to communication, while only a limited portion is reserved for synchronization. The synchronization signals, or pilots, are known to the receiver a priori, which enables opportunistic ranging and positioning [1]. Thus, a receiver estimates the distance, or range, to a transmitter by performing time-delay estimation (TDE) on the received signal. The most common method, known as single-path maximum-likelihood estimation (MLE), involves cross-correlating the received pilot signal with a known replica of the transmitted pilot signal. Then, the time-delay is selected as the value that maximizes this correlation. Although the single-path MLE is computationally efficient, its performance can deteriorate significantly in multipath environments.

Multipath environments are filled with objects that reflect the transmitted signal, causing multiple copies of this signal to arrive at the receiver antenna via different paths. In a line-of-sight (LOS) scenario, the first and strongest component that arrives at the receiver is the direct path and the subsequent ones are multipath components caused by reflections. Multipath often causes an estimation bias. To reduce this bias, a receiver can jointly estimate all the paths L in the channel [2]. In practice, though, this is computationally intensive, and receivers can restrict the estimation model to account only for the dominant paths $\hat{L}$ [3]. Since the actual number of paths is typically unknown, the receiver must also determine how many paths to include—a process known as model order selection [4]. Underestimating the number of paths leads to model misspecification and can significantly degrade estimation performance.

Estimation with a misspecified model order not only leads to a bias but also results (with nonlinear models) in a variance that differs from the theoretically expected Cramér-Rao Bound (CRB) [5], [6]. In such cases, the misspecified Cramér-Rao Bound (MCRB) provides the proper lower bound on the variance, as it accounts for the discrepancy between the assumed and the true number of paths. Consequently, the overall performance, quantified by the mean square error (MSE), can be lower-bounded using the bias-variance decomposition with the variance given by the MCRB. This bias-variance decomposition provides a complete and realistic bound on the performance for misspecified estimation problems.

Although the MCRB has been used for time-delay estimation with GNSS applications under multipath scenarios [7], including meta-signals [8], it has not yet been adapted to OFDM. A key distinction lies in frequency synchronization. Unlike in GNSS, OFDM receivers generally compensate for carrier frequency offset and Doppler shift prior to performing range estimation. As a result, these impairments do not need to be estimated during the ranging process. Also, the performance measures introduced in this paper are generally applicable to an $\hat{L}$-path receiver in an L-path channel, where $\hat{L} < L$. While [7] and [8] were limited to analysing the performance for a few discrete combinations of delay and gain, this work provides a more comprehensive analysis by evaluating bias, variance and MSE as a function of the relative delay across different carrier phase differences. This allows us to determine whether the estimation variance is bounded by constructive and destructive multipath components, analogous to the well-characterized bound on the bias by the multipath error envelope (MPEE).

This paper derives bounds on time-delay estimation for OFDM systems using a frequency domain formulation of the measurement model, focusing on the scenario where the receiver underestimates the number of propagation paths. While this frequency domain framework can be generalized to other modulations, a time domain derivation is often more practical in these cases.

We analyse the bias, variance, and MSE under model misspecification. Our aim is two-fold: first, to quantify how a multipath component affects the estimator's variance, and second, to establish a lower bound on the MSE using the bias-variance decomposition for a generic L-path channel when the estimator considers fewer paths $\hat{L}$. To illustrate the impact on the estimator's variance due to a multipath component not considered by the receiver, we analyse the MCRB for a two-path channel as a function of the delay separation between the paths, considering constructive, destructive, and other values of carrier phase differences. Employing a deterministic instead of a Bayesian channel model, enables us to explicitly isolate and analyse the effect on estimation bias and variance for different relative carrier phases between multipath components. Additionally, modelling the paths with deterministic delays allows us to analyse the estimator performance as a function of the relative delays. This is important because it reveals interactions that can significantly degrade or even improve estimator performance—these effects are inherently averaged out in a Bayesian framework. Finally, we compare the MSE bound with the empirical performance obtained with a simulated six-path channel frequency response with fixed path delays and gains, for a range of signal-to-noise ratios (SNRs). Our analysis provides a fundamental understanding of the impact of multipath on time-delay estimation, which is critical for the design and development of robust ranging systems.

The contributions of this work are:

- A semi-closed form expression for the MCRB of the TDE estimator when the user assumes a single-path estimator $\hat{L} = 1$, but the channel contains L deterministic propagation paths.
- A general expression for the MCRB of the TDE estimator which accounts for $\hat{L} < L$ paths, where L is the total number of paths in the channel.
- An assessment of the MSE bound's tightness using a simulated six-path channel, evaluating the empirical MSE for an $\hat{L}$-path estimator with $\hat{L} = 1, \cdots, 6$.

II. BACKGROUND

For ranging in multipath channels, only the first arriving path is of interest, while the reflected components, when included in the data model, act as nuisance parameters. Although the receiver is not interested in the nuisance parameters, they are present in the received signal and therefore influence the estimator's performance. In the literature, lower bounds on estimation performance are typically derived by considering the joint estimation of both the desired and nuisance parameters, as in the modified CRB [9], [10]. In contrast, here, only a subset of the parameters is jointly estimated, while the remaining parameters are neglected.

Depending on the receiver's prior statistical knowledge about the unknown parameters, statistical bounds can be classified as deterministic, Bayesian, or hybrid. Deterministic bounds such as the deterministic CRB [11], and Barankin bound [12] assume no prior knowledge of the unknown parameters. The deterministic CRB is simple to apply and often yields an intuitive, closed-form analytic expression. This simplicity comes at a cost: the bound is not global. The CRB is too optimistic at low SNRs, as it ignores the thresholding effect. This phenomenon arises from the nonlinear nature of time-delay estimation, where an estimator may lock onto a sidelobe of the autocorrelation function, leading to large estimation errors not captured by the CRB. Del Peral-Rosado et al. derived the CRB for the joint estimation of delays and gains of all paths [2]. Similarly, in the case of two-path channels with real-valued gains, Dun et al. presented an analytical approximation for the CRB of the joint estimation of delay and gain [13]. Wang et al. in [14] derived the CRB for both deterministic multipath channels and Bayesian channels, the latter obtained by modelling the channel gains as random variables.

Bayesian bounds, such as the Bayesian CRB [15] and Ziv-Zakai bound (ZZB) [16], [17], are applicable when the receiver has prior knowledge of the statistical distribution of all unknown parameters. Contrary to the Bayesian CRB, the ZZB is a global bound which considers the thresholding effect. However, the ZZB is difficult to interpret, requiring the numerical computation of several integrals. Where the Bayesian CRB is computationally intractable, other bounds such as the modified CRB offer a more feasible alternative, though it yields a looser bound [9], [10]. For instance, Graff et al. obtained the ZZB for a Rayleigh fading channel, considering both a receiver with perfect knowledge of the channel gains, and a receiver with knowledge limited to the fading distribution [18].

When some of the parameters are deterministic, and others are Bayesian, hybrid bounds can be used [19]. Alternatively, other bounds on the MSE performance for maximum likelihood estimators can be obtained by approximating the estimator's statistics using the Method of Interval Estimation (MIE) [20].

All the aforementioned bounds apply to an unbiased receiver that jointly estimates the unknown parameters, namely the delay and gain of all paths. This corresponds to the case in which the estimator uses a parameterized model of the true distribution of the channel frequency response. Here, however, we deal with a different problem. We want to assess the performance of a simplified receiver that considers less paths than present. This scenario is useful for analysing the impact of multipath on time-delay estimation when multipath is not accounted for.

In this paper, the unknown parameters in the estimation model, i.e., delay and complex propagation gain of each path are modelled as deterministic, to reflect a receiver model that does not assume any prior statistical knowledge of the channel as it is unaware of multipath propagation. Considering fewer signal paths implies that the channel model assumed by the receiver is different from the true model, i.e., the receiver is using a misspecified model. Misspecification introduces a bias, and the estimation variance deviates from that predicted by the CRB.

The misspecified CRB provides a lower limit on the estimation variance for misspecified estimators that model the unknown parameters as deterministic. This is different from the Bayesian ZZB, which offers a bound on the total MSE. While the ZZB can, in principle, be applied to scenarios with model mismatches [21], the MCRB offers a significant advantage as it provides tractable and easier expressions than the ZZB. In the case of multipath propagation, we define an estimator as misspecified if it considers an incorrect (lower) number of paths. The performance of the misspecified estimator was first analysed by Huber [22], Akaike [23], and White [24]. Later, Richmond and Horowitz [5], and Stefano Fortunati et al. [6] derived a bound on the variance of the misspecified estimator, namely the MCRB.

The MCRB framework has been applied for direction of arrival (DOA) estimation in MIMO radar systems when the estimator ignores the multipath components in a two-path channel [25], in 5G/6G positioning under hardware impairments [26], and localization with intelligent surfaces (RIS) under geometry mismatch [27]. Additionally, this bound has been applied to the joint misspecified delay-Doppler estimation problem for the GPS L1 C/A signal in the presence of multipath [7], which was recently extended for GNSS meta-signals [8]. However, the MCRB has not yet been applied in OFDM-based ranging to quantify the effect of multipath on the variance.

In this work, we do not address the uncertainty associated with the model order estimation procedure itself [28]. Instead, we assume a fixed, underestimated or equal number of paths at the receiver. This choice is motivated by practical ranging and positioning systems, where time-delay estimation is typically performed in real-time, and computational constraints often lead to the adoption of simplified estimation models in which not all the paths are estimated. Our focus is on characterizing the bias and variance induced by unmodelled deterministic multipath components when a reduced model order is intentionally used.

Notation: $\mathbb{E}\{\cdot\}$ denotes the expectation operation. $\Re\{\cdot\}$ and $\Im\{\cdot\}$ denote the real and imaginary part of a complex variable, respectively. $\mathbb{R}^{N\times L}$ and $\mathbb{C}^{N\times L}$ denote real and complex matrices with N rows and L columns, respectively. Uppercase boldface letters (e.g., $\mathbf{A}$) are used for matrices, and lowercase boldface letters (e.g., $\mathbf{h}$) are used for column vectors, and lowercase regular letters (e.g., $\boldsymbol{\tau}$) are used for scalars. $\mathbf{0}_N^T$ and $\mathbf{1}_N^T$ denote row vectors of length N, with all the entries equal to 0 and 1, respectively, while $\mathbf{0}_{N\times N}$ and $\mathbf{1}_{N\times N}$ denote $N \times N$ matrices of all zeros and all ones, respectively. An identity matrix of dimension N is denoted by $\mathbf{I}_N$. $\underline{()}$ denotes a random variable, $\hat{()}$ denotes an estimate, $\underline{\hat{()}}$ denotes an estimator, and $()^T$, $()^*$, $()^H$, denote the transpose, conjugate and Hermitian transpose, respectively. diag$(\cdot)$ denotes the diagonal matrix with its vector argument on the main diagonal. Operators $\odot$, $\times$ and $|\cdot|$ denote the element-wise product, the Cartesian product and the absolute value of a complex number, respectively. The term $||\mathbf{v}||^2_{\mathbf{Q}_\mathbf{h}^{-1}}$ denotes the squared weighted norm of $\mathbf{v}$, and is computed as $\mathbf{v}^H\mathbf{Q}_\mathbf{h}^{-1}\mathbf{v}$.

III. SIGNAL MODEL

We consider an OFDM transmission scheme and a receiver which measures the channel frequency response (CFR) $\mathbf{h}$ based on known transmitted symbols. The CFR is obtained per-sub-carrier following a least-squares decision-directed channel estimation approach as described in [3], [13], and [29]. Accordingly, the vector collecting the CFR estimates in baseband over N_s sub-carriers can be written as

$$\begin{aligned}\underline{\mathbf{h}} &= \underline{\mathbf{s}}_{rx} \odot \frac{1}{\mathbf{s}_{tx}} \\ &= \mathbf{h} + \underline{\mathbf{w}} \odot \frac{1}{\mathbf{s}_{tx}} = \mathbf{h} + \underline{\mathbf{n}},\end{aligned} \tag{1}$$

where $\underline{\mathbf{s}}_{rx} = \mathbf{s}_{tx} \odot \mathbf{h} + \underline{\mathbf{w}}$ denotes the vector containing the received baseband symbols in the frequency domain, and $\mathbf{s_{tx}}$ denotes the known transmitted symbols. The noise component in $\mathbf{s}_{rx}$ is modelled as $\underline{\mathbf{w}} \sim \mathcal{CN}_{N_s}(\mathbf{0}_{N_s}, \sigma_n^2\mathbf{I}_{N_s})$, which implies that

$$\underline{\mathbf{n}} \sim \mathcal{CN}_{N_s}\left(0, \sigma_n^2\,\mathrm{diag}\left(\frac{1}{\mathbf{s}_{tx} \odot \mathbf{s}_{tx}^*}\right)\right). \tag{2}$$

The notation $\mathcal{CN}_{N_s}(\boldsymbol{\mu}, \mathbf{Q_h})$ denotes an N_s-dimensional complex Gaussian distribution with mean $\boldsymbol{\mu}$ and variance matrix $\mathbf{Q_h}$. For simplicity and ease of notation we consider that $\mathbf{s}_{tx}$ is BPSK modulated, so that $\mathbf{s}_{tx} \odot \mathbf{s}_{tx}^* = \mathbf{1}_{N_s}$, where $\mathbf{1}_{N_s}$ is an N_s-column vector with all ones, and thus $\underline{\mathbf{n}} \sim \mathcal{CN}_{N_s}\left(\mathbf{0}_{N_s}, \sigma_n^2\mathbf{I}_{N_s}\right)$.

In an L-path channel, the CFR in baseband can be modelled as

$$\underline{\mathbf{h}} = \sum_{l=1}^{L} x_l \exp(-j2\pi\mathbf{f}\tau_l) + \underline{\mathbf{n}}, \quad \underline{\mathbf{n}} \sim \mathcal{CN}_{N_s}(\mathbf{0}_{N_s}, \sigma_n^2\mathbf{I}_{N_s}), \tag{3}$$

where τ_l and x_l are the l-th path residual propagation time-delay after symbol synchronization and complex propagation gain, respectively. The vector $\mathbf{f}$ contains N_s sub-carrier frequencies used for ranging, and $\underline{\mathbf{n}}$ is a vector containing additive white Gaussian noise (AWGN).

Based on least-squares channel estimation (1), the measurement model in the frequency domain for time-delay estimation in an L-path deterministic propagation channel becomes [3], [13]:

$$\begin{aligned}\underline{\mathbf{h}} &\sim \mathcal{CN}_{N_s}(\mathbb{E}\left\{\underline{\mathbf{h}}\right\}, \mathbf{Q_h}), \\ \mathbb{E}\left\{\underline{\mathbf{h}}\right\} &= \mathbf{A}(\boldsymbol{\tau})\mathbf{x}, \quad \mathbf{Q_h} = \sigma_n^2\mathbf{I}_{N_s},\end{aligned} \tag{4}$$

where

$$\begin{aligned}\mathbf{A}(\boldsymbol{\tau}) &= \left[\mathbf{a}(\tau_1)\ \mathbf{a}(\tau_2)\ \cdots\ \mathbf{a}(\tau_L)\right] \in \mathbb{C}^{N_s\times L}, \\ \mathbf{a}(\tau_l) &= \exp(-j2\pi\mathbf{f}\tau_l) \in \mathbb{C}^{N_s\times 1}, \\ \boldsymbol{\tau} &= \left[\tau_1\ \tau_2\ \cdots\ \tau_L\right]^T \in \mathbb{R}^{L\times 1}, \\ \mathbf{x} &= \left[x_1\ x_2\ \cdots\ x_L\right]^T \in \mathbb{C}^{L\times 1}, \\ \mathbf{f} &= \left[f_1\ f_2\ \cdots\ f_{N_s}\right]^T \in \mathbb{R}^{N_s\times 1},\end{aligned} \tag{5}$$

and $\mathbf{h} \in \mathbb{C}^{N_s\times 1}$ is a vector containing the measured channel frequency response at the N_s sub-carrier frequencies in $\mathbf{f}$; $\boldsymbol{\tau}$ and $\mathbf{x}$ are vectors containing the unknown, deterministic delays and complex propagation gains of the L signal paths. Note that $L < N_s$, and typically $L \ll N_s$.

$\mathbf{Q_h}$ is the variance matrix of the CFR and we assume it is scaled identity, i.e., the noise variance is identical across all sub-carriers and there is no covariance between different sub-carriers. This is justified because the least-squares channel estimator (1) does not color the noise, unlike pilot-aided approaches [30]. Additionally, modelling each path as deterministic does not introduce any noise coloring.

To simplify the notation, we express the expectation of the channel frequency response as a function of the unknown parameter vector $\boldsymbol{\theta}$ as:

$$\mathbb{E}\left\{\underline{\mathbf{h}}\right\} = \boldsymbol{\mu}(\boldsymbol{\theta}) = \mathbf{A}\left(\begin{bmatrix}\tau_1\\ \vdots \\ \tau_L\end{bmatrix}\right)\begin{bmatrix}\Re\{x_1\} + j\Im\{x_1\}\\ \vdots \\ \Re\{x_L\} + j\Im\{x_L\}\end{bmatrix}, \tag{6}$$

where

$$\boldsymbol{\theta} = \left[\boldsymbol{\tau}^T\ \Re\{\mathbf{x}^T\}\ \Im\{\mathbf{x}^T\}\right]^T \in \mathbb{R}^{3L\times 1}. \tag{7}$$

By stacking the real and imaginary parts of the complex gains, all elements of the unknown parameter vector become real-valued, which simplifies the calculus involved in our derivations. It is also possible to consider $\mathbf{x}$ as complex-valued, in which case the computation of the CRB and MCRB requires the use of Wirtinger calculus [5].

Based on the measurement model (4) and the maximum likelihood estimation (MLE) principle, we can estimate the delays $\boldsymbol{\tau}$ and complex gains $\mathbf{x}$ by minimizing the following weighted nonlinear least squares (NLS) problem with weighting matrix $\mathbf{Q}_\mathbf{h}^{-1}$:

$$\begin{bmatrix}\hat{\boldsymbol{\tau}}\\ \hat{\mathbf{x}}\end{bmatrix} = \arg\min_{\boldsymbol{\tau},\mathbf{x}} ||\mathbf{h} - \mathbf{A}(\boldsymbol{\tau})\mathbf{x}||^2_{\mathbf{Q}_\mathbf{h}^{-1}}. \tag{8}$$

We can express the minimization problem (8) as a function of the delays alone, by decoupling the estimation of the delays and the gains [31]

$$\hat{\boldsymbol{\tau}} = \arg\min_{\boldsymbol{\tau}} ||\mathbf{h} - \mathbf{A}(\boldsymbol{\tau})\hat{\mathbf{x}}||^2_{\mathbf{Q}_\mathbf{h}^{-1}}, \tag{9}$$

where the estimated gains are expressed as

$$\hat{\mathbf{x}} = \left(\mathbf{A}^H(\boldsymbol{\tau})\mathbf{Q}_\mathbf{h}^{-1}\mathbf{A}(\boldsymbol{\tau})\right)^{-1}\mathbf{A}^H(\boldsymbol{\tau})\mathbf{Q}_\mathbf{h}^{-1}\mathbf{h}. \tag{10}$$

The decoupling step can be done if $\text{rank}(\mathbf{A}(\boldsymbol{\tau})) = L$, which implies that matrix $\mathbf{A}^H(\boldsymbol{\tau})\mathbf{Q}_\mathbf{h}^{-1}\mathbf{A}(\boldsymbol{\tau})$ is invertible. This condition requires that the path delays are non-degenerate, implying that very closely spaced multipath cannot be resolved.

Additionally, a set of delays $\hat{\boldsymbol{\tau}}$ is a minimizer of the NLS problem in (9) if and only if the first- and second-order derivatives of the associated cost function satisfy [32]:

$$\frac{\partial(\mathbf{h} - \mathbf{A}(\hat{\boldsymbol{\tau}})\hat{\mathbf{x}})}{\partial\boldsymbol{\tau}} = 0, \quad \frac{\partial^2(\mathbf{h} - \mathbf{A}(\hat{\boldsymbol{\tau}})\hat{\mathbf{x}})}{\partial\boldsymbol{\tau}\partial\boldsymbol{\tau}^T} > 0. \tag{11}$$

The optimization problem in (9) can be expressed by

$$\hat{\boldsymbol{\tau}} = \arg\min_{\boldsymbol{\tau}} ||P^{\perp}_{A(\tau)}\mathbf{h}||^2_{\mathbf{Q}_\mathbf{h}^{-1}}, \tag{12}$$

where the projection and orthogonal projection matrices are defined by

$$\begin{aligned} P_{A(\tau)} &= \mathbf{A}(\boldsymbol{\tau})\left(\mathbf{A}^H(\boldsymbol{\tau})\mathbf{Q}_\mathbf{h}^{-1}\mathbf{A}(\boldsymbol{\tau})\right)^{-1}\mathbf{A}^H(\boldsymbol{\tau})\mathbf{Q}_\mathbf{h}^{-1}, \\ P^{\perp}_{A(\tau)} &= \mathbf{I}_{N_s} - P_{A(\tau)}, \end{aligned} \tag{13}$$

where $\mathbf{I}_{N_s}$ is a $N_s \times N_s$ identity matrix.

In the following sections we derive bounds for the bias, variance and MSE on the time-delay estimator of the first path $\hat{\tau}_1$. These bounds are independent of the estimation method used. However, the MLE principle, shown in (8) for TDE, is of special interest as it is asymptotically unbiased and efficient. Thus, for high SNRs, estimators based on MLE are unbiased and attain the CRB [11]. This also holds for the multi-parameter case [33].

IV. CRB

The variance of an unbiased estimator is lower bounded by the Cramér-Rao bound (CRB). Consider an L-path channel and a receiver that jointly estimates the delays and gains of all the paths. Then, the variance of the estimated delay of the first path is obtained by [11]

$$\sigma^2_{\hat{\tau}_1} \geq [(\mathbf{FIM}(\boldsymbol{\theta}))^{-1}]_{1,1}, \tag{14}$$

where each element of the $3L \times 3L$ Fisher information matrix $\mathbf{FIM}(\boldsymbol{\theta})$ is obtained as

$$\begin{aligned} [\mathbf{FIM}(\boldsymbol{\theta})]_{i,k} = \text{tr}&\left[\mathbf{Q}_\mathbf{h}^{-1}(\boldsymbol{\theta})\frac{\partial\mathbf{Q}_\mathbf{h}(\boldsymbol{\theta})}{\partial\theta_i}\mathbf{Q}_\mathbf{h}^{-1}(\boldsymbol{\theta})\frac{\partial\mathbf{Q}_\mathbf{h}(\boldsymbol{\theta})}{\partial\theta_k}\right] \\ &+ 2\,\Re\left[\frac{\partial\boldsymbol{\mu}^H(\boldsymbol{\theta})}{\partial\theta_i}\mathbf{Q}_\mathbf{h}^{-1}(\boldsymbol{\theta})\frac{\partial\boldsymbol{\mu}(\boldsymbol{\theta})}{\partial\theta_k}\right]. \end{aligned} \tag{15}$$

Note that in our case, since the a-priori set variance matrix $\mathbf{Q}_\mathbf{h} = \sigma_n^2\mathbf{I}_{N_s}$ does not depend on $\boldsymbol{\theta}$, the first term of (15) vanishes. Therefore, the FIM can be expressed as

$$\mathbf{FIM}(\boldsymbol{\theta}) = \frac{2}{\sigma_n^2}\Re\left[\left(\frac{\partial\boldsymbol{\mu}(\boldsymbol{\theta})}{\partial\boldsymbol{\theta}^T}\right)^H\frac{\partial\boldsymbol{\mu}(\boldsymbol{\theta})}{\partial\boldsymbol{\theta}^T}\right], \tag{16}$$

where $\boldsymbol{\theta}$ is the vector of unknown parameters (7), and $\frac{\partial\boldsymbol{\mu}(\boldsymbol{\theta})}{\partial\boldsymbol{\theta}^T}$ is the Jacobian matrix of the expectation of the channel frequency response $\boldsymbol{\mu}(\boldsymbol{\theta})$, defined in (6). The Jacobian matrix can be computed as in (63).

In the following, we derive the CRB on the time-delay estimator of the first path in a single-path channel and in an L-path channel under additive white Gaussian noise (AWGN). The Fisher information matrix of subsections IV-A and IV-B is obtained based on Appendix B.

A. CRB FOR 1-PATH MLE

In the simple case of a single-path AWGN channel ($L = 1$), the variance of the TDE estimator is lower bounded by [2]

$$\boxed{\sigma^2_{\text{CRB}} = \frac{\sigma_n^2}{8\pi^2|x_1|^2\mathbf{f}^T\mathbf{f}}}, \tag{17}$$

where $|x_1|^2/\sigma_n^2$ is the SNR, and σ_n^2 is the noise power per sub-carrier, for all sub-carriers contained in (4).

The same bound is achieved whether the gain is jointly estimated with the delay or treated as an unknown parameter without explicit estimation. Additionally, note that (17) does not depend on the carrier phase of the received signal.

The variance of the time-delay estimator is inversely proportional to the curvature of the mainlobe of the band-limited signal's autocorrelation function (ACF) [34, p. 104]. Specifically,

$$\sigma^2_{\text{CRB}} = \frac{\sigma_n^2}{-2|x_1|^2R_s''(0)} \propto \frac{1}{-R_s''(0)}, \tag{18}$$

where the ACF is defined using the frequency domain formulation as

$$R_s(\tau) = \mathbf{a}^H(\tau_1)\mathbf{a}(\tau_1 + \tau) = \mathbf{1}_{N_s}^T\mathbf{a}(\tau), \tag{19}$$

The first and second derivatives of $R_s(\tau)$ are given in Appendix C.

Note that the mainlobe of the autocorrelation is concave, so its second derivative is negative. With expression (18), we see that a large negative value of the second derivative of the mainlobe of the ACF is desirable, as it corresponds to a sharper peak and thus improves the precision of the time-delay estimator.

B. CRB FOR L-PATH MLE

The Fisher information matrix for the joint estimation of L paths in AWGN with unknown parameter vector $\boldsymbol{\theta}$ defined in (7), is expressed as [2]

$$\mathbf{FIM}(\boldsymbol{\theta}) = \frac{2}{\sigma_n^2}\begin{bmatrix}\mathbf{FIM}_{\boldsymbol{\tau}} & \mathbf{FIM}_{\boldsymbol{\tau}\mathbf{x}} \\ \mathbf{FIM}_{\mathbf{x}\boldsymbol{\tau}} & \mathbf{FIM}_{\mathbf{x}}\end{bmatrix}, \tag{20}$$

where

$$\begin{aligned}\mathbf{FIM}_{\boldsymbol{\tau}} &= 4\pi^2\Re\{\mathrm{diag}(\mathbf{x}^*)[(\mathbf{A}\odot\mathbf{F})^H(\mathbf{A}\odot\mathbf{F})]\,\mathrm{diag}(\mathbf{x})\},\\ \mathbf{FIM}_{\mathbf{x}} &= \begin{bmatrix}\Re\{\mathbf{A}^H\mathbf{A}\} & -\Im\{\mathbf{A}^H\mathbf{A}\}\\ \Im\{\mathbf{A}^H\mathbf{A}\} & \Re\{\mathbf{A}^H\mathbf{A}\}\end{bmatrix},\\ \mathbf{FIM}_{\mathbf{x}\boldsymbol{\tau}} &= \mathbf{FIM}_{\boldsymbol{\tau}\mathbf{x}}^T = 2\pi\begin{bmatrix}\Im\{(\mathbf{A}^H(\mathbf{A}\odot\mathbf{F}))\,\mathrm{diag}(\mathbf{x})\}\\ -\Re\{(\mathbf{A}^H(\mathbf{A}\odot\mathbf{F}))\,\mathrm{diag}(\mathbf{x})\}\end{bmatrix},\end{aligned} \tag{21}$$

where $\mathbf{A} = \mathbf{A}(\boldsymbol{\tau})$ is the matrix defined in (5), with the argument $\boldsymbol{\tau}$ omitted for compactness, and vector $\mathbf{x}$ contains the complex gains of the L paths. $\mathbf{F}$ is a matrix with L columns, each column containing the sub-carrier frequencies $\mathbf{f}$ previously defined in (5), that is

$$\mathbf{F} = \mathbf{f}\,\mathbf{1}_L^T \in \mathbb{R}^{N_s\times L}. \tag{22}$$

The dimensions of the matrices in (20) and (21) are given by $\mathbf{FIM}(\boldsymbol{\theta}) \in \mathbb{R}^{3L\times 3L}$, $\mathbf{FIM}_{\boldsymbol{\tau}} \in \mathbb{R}^{L\times L}$, $\mathbf{FIM}_{\mathbf{x}} \in \mathbb{R}^{2L\times 2L}$, and $\mathbf{FIM}_{\mathbf{x}\boldsymbol{\tau}} \in \mathbb{R}^{2L\times L}$. Matrix $\mathbf{FIM}_{\boldsymbol{\tau}}$ represents the Fisher information matrix corresponding to the joint estimation of all path delays, assuming the complex gains are known.

As indicated in (14), the CRB of the first path time-delay estimator follows from inverting the FIM in (20) and (21) and taking the element (1, 1) of the resulting matrix.

In the following, we prove that for a two-path channel, when jointly estimating the delays and gains of both paths, the CRB for the time-delay estimator of the first path is identical for relative phases $\Delta\phi$ and $\Delta\phi+\pi$ between the complex gains x_1 and x_2.

Proposition: Consider the joint estimation of the time-delay and gain of all paths in a two-path channel. Let us express the complex propagation gain for each path in polar form as

$$x_1 = |x_1|\exp(j\phi_1), \quad x_2 = |x_2|\exp(j\phi_2) \tag{23}$$

where ϕ_1 and ϕ_2 are the carrier phases of the first and second path, respectively. Without loss of generality, we set $\phi_1 = 0$. The carrier phase of the second path is then defined relative to the first path as $\phi_2 = \Delta\phi = \phi_2 - \phi_1$.

Then, the CRB for the time-delay of the first path remains the same for $\Delta\phi$ and $\Delta\phi + \pi$.

Proof: Consider the following parameterization of $\mathbf{FIM}_{\boldsymbol{\tau}}$ and $\mathbf{FIM}_{\mathbf{x}\boldsymbol{\tau}}$ in (20) in a two-path channel ($L = 2$):

$$\begin{aligned}\mathbf{FIM}_{\boldsymbol{\tau}} &= \mathbf{B} = \begin{bmatrix}b_{11} & b_{12}\\ b_{21} & b_{22}\end{bmatrix}\\ &= 4\pi^2\Re\{\begin{bmatrix}|x_1|^2\mathbf{f}^T\mathbf{f} & x_1^H x_2(\mathbf{f}^2)^T\mathbf{a}(\tau_{21})\\ x_2^H x_1(\mathbf{f}^2)^T\mathbf{a}(\tau_{12}) & |x_2|^2\mathbf{f}^T\mathbf{f}\end{bmatrix}\},\\ \mathbf{FIM}_{\mathbf{x}\boldsymbol{\tau}} &= \mathbf{R} = \begin{bmatrix}\mathbf{r}_1 & \mathbf{r}_2\end{bmatrix}\\ &= 2\pi\begin{bmatrix}\Im\{|x_1|\mathbf{f}^T\mathbf{1}_{N_s}\} & \Im\{|x_2|e^{j\Delta\phi}\mathbf{f}^T\mathbf{a}(\tau_{21})\}\\ \Im\{|x_1|\mathbf{f}^T\mathbf{a}(\tau_{12})\} & \Im\{|x_2|e^{j\Delta\phi}\mathbf{f}^T\mathbf{1}_{N_s}\}\\ -\Re\{|x_1|\mathbf{f}^T\mathbf{1}_{N_s}\} & -\Re\{|x_2|e^{j\Delta\phi}\mathbf{f}^T\mathbf{a}(\tau_{21})\}\\ -\Re\{|x_1|\mathbf{f}^T\mathbf{a}(\tau_{12})\} & -\Re\{|x_2|e^{j\Delta\phi}\mathbf{f}^T\mathbf{1}_{N_s}\}\end{bmatrix},\end{aligned} \tag{24}$$

where $\tau_{21} = \tau_2 - \tau_1$, and $\tau_{12} = \tau_1 - \tau_2$. Note that the following terms do not depend on the relative carrier phase $\Delta\phi$: scalars b_{11} and b_{22}, vector $\mathbf{r}_1$, and matrix $\mathbf{FIM}_{\mathbf{x}}$ defined in (21).

The inverse of $\mathbf{FIM}(\boldsymbol{\theta})$ is expressed as

$$\mathbf{FIM}^{-1}(\boldsymbol{\theta}) = \frac{\sigma_n^2}{2}\begin{bmatrix}\mathbf{J}_{\boldsymbol{\tau}} & \mathbf{J}_{\boldsymbol{\tau}\mathbf{x}}\\ \mathbf{J}_{\mathbf{x}\boldsymbol{\tau}} & \mathbf{J}_{\mathbf{x}}\end{bmatrix}, \tag{25}$$

where $\mathbf{J}_{\boldsymbol{\tau}}$ is a 2×2 matrix obtained as

$$\mathbf{J}_{\boldsymbol{\tau}} = (\mathbf{B} - \mathbf{R}^T\mathbf{S}\mathbf{R})^{-1}, \tag{26}$$

where $\mathbf{B}$ and $\mathbf{R}$ are defined in (24) and $\mathbf{S} = \mathbf{FIM}_{\mathbf{x}}^{-1}$.

Then, the CRB of the first path time-delay estimator corresponds to element (1, 1) of the matrix $\mathbf{J}_{\boldsymbol{\tau}}$. Expanding (26), the CRB for the first path estimator can be expressed as

$$\sigma^2_{\mathrm{CRB}} = \frac{\mathbf{r}_2^T\mathbf{S}\mathbf{r}_2}{(\mathbf{r}_1^T\mathbf{S}\mathbf{r}_1)(\mathbf{r}_2^T\mathbf{S}\mathbf{r}_2) - (b_{21} - \mathbf{r}_2^T\mathbf{S}\mathbf{r}_1)(b_{12} - \mathbf{r}_1^T\mathbf{S}\mathbf{r}_2)}. \tag{27}$$

Note that the following relations hold when applying a phase shift of π to the carrier phase difference $\Delta\phi$:

$$\begin{aligned}\mathbf{r}_2(\Delta\phi) &= -\mathbf{r}_2(\Delta\phi+\pi),\\ b_{21}(\Delta\phi) &= -b_{21}(\Delta\phi+\pi),\\ b_{12}(\Delta\phi) &= -b_{12}(\Delta\phi+\pi).\end{aligned} \tag{28}$$

Therefore, the CRB of the time-delay estimator (27) evaluated at $\sigma^2_{\tau_1}(\Delta\phi)$ is equal to $\sigma^2_{\tau_1}(\Delta\phi+\pi)$.

Note that the relation $|x_2|\exp(j\Delta\phi) = -|x_2|\exp(j(\Delta\phi+\pi))$ implies that a phase shift of π rad is equivalent to a sign inversion of the complex amplitude. Since this gives no new information about the amplitude, the matrix $\mathbf{J}_{\boldsymbol{\tau}}$ in (26) remains the same for $\Delta\phi$ and $\Delta\phi+\pi$, leading to the same CRB. □

This proof shows that the estimation variance of the first path remains the same for constructive and destructive multipath.

Figure 1 shows the CRB of the time-delay estimator in a two-path channel ($\hat{L} = L = 2$) as a function of the relative distance $c\tau_{21}$ between the paths, where c is the speed of light. The CRB is obtained with (20) for an OFDM signal with a 160 MHz bandwidth, which consists of 1024 sub-carriers separated by 156.25 kHz (Table 1). The SNR of the first path is set to 10 dB, the gains are $x_1 = 1$, and $x_2 = 0.7\exp(j\Delta\phi)$, where $\Delta\phi$ is the carrier phase difference between the paths. Observing this example, for all relative distances, the CRB is maximum when the second path arrives with the same phase as the first path, i.e., $\Delta\phi = 0$ (blue curve), and the minimum CRB is obtained when $\Delta\phi = \pi/2$ (yellow curve). Intuitively, when $\Delta\phi = \pi/2$, the gains x_1 and x_2 are orthogonal. This makes the two paths easier to distinguish and thereby reduces the variance of the first path's time-delay estimator. Conversely, when $\Delta\phi = 0$, the gains become coherent, making it more difficult to separate the two paths, leading to an increased variance for the first path's time-delay estimator.

TABLE 1. OFDM simulation parameters used in figs. 1, 2, 3, 4, 5, 6, and 8.

Bandwidth [B]	160 MHz
Sub-carrier spacing	156.25 kHz
Number of sub-carriers	1024
Gain of first path (absolute value) $\lvert\alpha_1\rvert$	1
Gain of second path (absolute value) $\lvert\alpha_2\rvert$	0.7
SNR of first path	10 dB

V. MODEL MISSPECIFICATION

In practical estimation problems, it is common to rely on simplified or approximated models that may not capture the entire complexity of the underlying process. For instance, in TDE, one might assume a single propagation path while neglecting the multipath components. When the estimation algorithm assumes a model different from the true one, *model misspecification* occurs [5]. An estimator that is based on a misspecified model is known as a *misspecified estimator* [6].

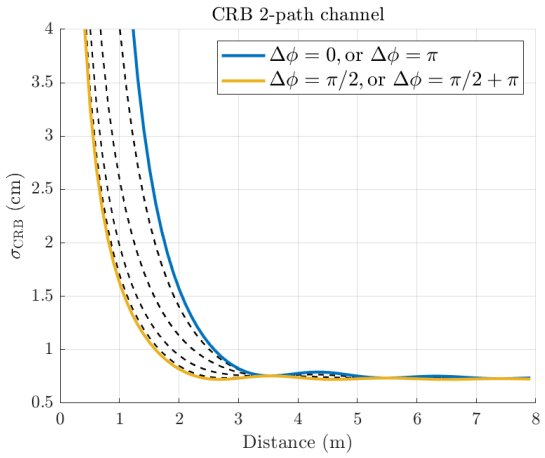

FIGURE 1. Square root of the CRB of the time-delay estimator of the first path in a two-path channel, plotted as a function of the path separation $c\tau_{21}$ (distance). Joint estimation of delays and gains of both paths is assumed. OFDM parameters are shown in table 1. Dashed black curves represent the CRB for different values of carrier phase difference $\Delta\phi \in [0, 2\pi]$.

Under model misspecification, the user believes that the channel frequency response (4) follows the distribution

$$\underline{\mathbf{h}} \sim f_{\underline{\mathbf{h}}}(\mathbf{h}|\boldsymbol{\theta}_{\text{user}}) = \mathcal{CN}_{N_s}(\boldsymbol{\mu}(\boldsymbol{\theta}_{\text{user}}), \mathbf{Q}_{\mathbf{h}}), \tag{29}$$

whereas the true distribution is

$$\underline{\mathbf{h}} \sim g_{\underline{\mathbf{h}}}(\mathbf{h}) = \mathcal{CN}_{N_s}(\mathbf{d}, \mathbf{Q}_{\mathbf{h}}). \tag{30}$$

Here we assume that the mismatch between the true and assumed model arises only in the expectation of the channel frequency response, while the variance matrix $\mathbf{Q}_{\mathbf{h}}$ remains the same. This assumption is justified by modelling the path delays and gains as deterministic; consequently any unmodelled multipath components in the assumed model affect only the mean of the CFR and do not alter its variance matrix. The vector of deterministic unknown parameters that the user estimates is $\boldsymbol{\theta}_{\text{user}} \in \mathbb{R}^{3\hat{L}}$ (7), where $\hat{L}$ is the number of paths considered by the user in the estimation model. $\hat{L}$ is not an estimate of the number of paths; the hat here indicates that it corresponds to the number of paths assumed in the estimation model. The total number of unknown parameters is $3\hat{L}$, as for each path the user jointly estimates the time-delay and real and imaginary parts of the complex propagation gain.

The user estimates the vector of unknown parameters $\boldsymbol{\theta}_{\text{user}}$ based on the misspecified distribution $f_{\underline{\mathbf{h}}}(\mathbf{h}|\boldsymbol{\theta}_{\text{user}})$. Under model misspecification, the estimator does not converge to the true parameter vector $\boldsymbol{\theta}_{\text{true}}$, but instead to the *pseudotrue* parameter vector $\boldsymbol{\theta}_0$. Estimators with this property are called misspecified-unbiased (*MS-unbiased*).

The pseudotrue parameter is defined as the value of $\boldsymbol{\theta}_{\text{user}}$ that minimizes the Kullback-Leibler divergence (KLD) between the true and assumed models:

$$\begin{aligned}\boldsymbol{\theta}_0 &= \arg\min_{\boldsymbol{\theta}_{\text{user}}} \left\{ D\left(g_{\underline{\mathbf{h}}}(\mathbf{h}) \| f_{\underline{\mathbf{h}}}(\underline{\mathbf{h}}|\boldsymbol{\theta}_{\text{user}})\right)\right\} \\ &= \arg\min_{\boldsymbol{\theta}_{\text{user}}} \left\{ \mathbb{E}_g\{\ln g_{\underline{\mathbf{h}}}(\underline{\mathbf{h}})\} - \mathbb{E}_g\left\{\ln f_{\underline{\mathbf{h}}}(\underline{\mathbf{h}}|\boldsymbol{\theta}_{\text{user}})\right\}\right\} \\ &= \arg\min_{\boldsymbol{\theta}_{\text{user}}} \left\{ -\mathbb{E}_g\left\{\ln f_{\underline{\mathbf{h}}}(\underline{\mathbf{h}}|\boldsymbol{\theta}_{\text{user}})\right\}\right\}. \end{aligned} \tag{31}$$

In this paper, we only consider TDE in the mid-to-high SNR regime. For large values of SNR and under the regularity conditions in [24], the misspecified maximum likelihood estimator (MML) $\hat{\underline{\boldsymbol{\theta}}}_{\text{MML}}$ is MS-unbiased and its error covariance matrix converges to the MCRB [6]:

$$\begin{aligned}\mathbb{E}_g\{\hat{\underline{\boldsymbol{\theta}}}_{\text{MML}} - \boldsymbol{\theta}_0\} &\to 0, \\ \mathbb{E}_g\{(\hat{\underline{\boldsymbol{\theta}}}_{\text{MML}} - \boldsymbol{\theta}_0)(\hat{\underline{\boldsymbol{\theta}}}_{\text{MML}} - \boldsymbol{\theta}_0)^T\} &\to \text{MCRB}(\boldsymbol{\theta}_0). \end{aligned} \tag{32}$$

In the case of model misspecification, we consider a scenario in which a receiver *underestimates* the number of paths, i.e., a user considers $\hat{L}$ paths, while in reality there are $L > \hat{L}$ in the channel. The distribution of the channel frequency response $\mathbf{h}$ can then be parameterized by the user-assumed model (29) as

$$\mathcal{F}_{\hat{L}} = \left\{ \mathcal{CN}_{N_s}(\boldsymbol{\mu}(\boldsymbol{\theta}_{\text{user}}), \mathbf{Q}_{\mathbf{h}}) \ : \ \boldsymbol{\theta}_{\text{user}} \in \Theta = \mathbb{R}^{3\hat{L}} \right\}, \tag{33}$$

and by the true model (30) which accounts for all the paths as

$$\mathcal{G}_L = \left\{ \mathcal{CN}_{N_s}(\boldsymbol{\mu}(\boldsymbol{\theta}_{\text{true}}, \boldsymbol{\gamma}), \mathbf{Q}_{\mathbf{h}}) : \forall(\boldsymbol{\theta}_{\text{true}}, \boldsymbol{\gamma}) \in \Theta \times \Gamma = \mathbb{R}^{3L} \right\}, \tag{34}$$

where $\boldsymbol{\mu}(\boldsymbol{\theta}_{\text{true}}, \boldsymbol{\gamma}) = \mathbf{d}$ in (30), and $\boldsymbol{\gamma} \in \Gamma = \mathbb{R}^{3(L-\hat{L})}$ is the vector of additional parameters associated with the $L - \hat{L}$ paths omitted in the user-assumed model.

In this paper, the expectation of the CFR is treated as deterministic. Accordingly, we define $\boldsymbol{\theta}_{\text{true}}$ as the true deterministic parameter vector the user aims to estimate, and express the expectation of $\underline{\mathbf{h}}$ under the true distribution as $\mathbf{d} = \boldsymbol{\mu}(\boldsymbol{\theta}_{\text{true}}, \boldsymbol{\gamma})$, where $\mathbf{d}$ denotes the mean of the complex Gaussian model in (30). $\boldsymbol{\theta}_{\text{true}}$ is organized in a vector whose size and structure correspond to the parameter vector that the user estimates $\boldsymbol{\theta}_{\text{user}}$.

The parameters of the true distribution can be expressed with (7) as

$$\begin{aligned}\boldsymbol{\theta}_{\text{true}} &= \left[\tau_1, ..., \tau_{\hat{L}}, \Re\{x_1\}, ..., \Re\{x_{\hat{L}}\}, \Im\{x_1\}, ..., \Im\{x_{\hat{L}}\}\right]^T, \\ (\boldsymbol{\theta}_{\text{true}}, \boldsymbol{\gamma}) &= \left[\tau_1, ..., \tau_L, \Re\{x_1\}, ..., \Re\{x_L\}, \Im\{x_1\}, ..., \Im\{x_L\}\right]^T,\end{aligned} \tag{35}$$

where τ_i is the true delay of the i-th path, and $\Re\{x_i\}$ and $\Im\{x_i\}$ are the real and imaginary parts of the complex gain x_i, respectively, as defined in (7), representing the actual parameter values of the CFR.

Since $\hat{L} < L$, the user-assumed model is *nested* in the true model. This holds because the parameter space of the user-assumed model $\mathcal{F}_{\hat{L}}$, given by $\boldsymbol{\theta}_{\text{user}} \in \mathbb{R}^{3\hat{L}}$, can be extended with a zero vector $\mathbf{0}_{3(L-\hat{L})}$ to form $(\boldsymbol{\theta}_{\text{user}}, \mathbf{0}_{3(L-\hat{L})}) \in \mathbb{R}^{3L}$. This extended vector is a subspace of the parameter space of the true model $\mathcal{G}_L$, given by $(\boldsymbol{\theta}_{\text{true}}, \boldsymbol{\gamma})$.

In the following sections, we derive estimation bounds on the bias, variance and MSE of the time-delay estimator for the first arriving path, for the scenario where the user considers fewer signal paths than actually present.

VI. ESTIMATION BIAS

When the estimation model does not account for all the multipath components present in the channel frequency response, the resulting estimator may be biased.

To quantify the time-delay estimation bias we consider two approaches: (i) analytical approximation [13], where a closed-form expression is derived by approximating the MLE cost function (9); and (ii) numerical computation [35], where the bias is obtained by numerically estimating the pseudotrue parameter $\boldsymbol{\theta}_0$ (31).

The approximate closed-form expressions are provided to offer qualitative insight; however, in the numerical simulations in Section IX, the bias is evaluated without approximation using numerical computation (Subsection VI-B).

A. ESTIMATION BIAS VIA ANALYTICAL APPROXIMATION

In the first approach, time-delay estimation bias due to an unconsidered reflection in a two-path channel is obtained by linearizing (9) at the true delay τ_1 for $\hat{L} = 1, L = 2$, neglecting the second and higher order terms [13]. This yields

$$\tau_b \approx \Re\left\{\frac{j\pi x_1^H x_2 \mathbf{f}^T \mathbf{a}\,(\tau_2 - \tau_1)}{2\pi^2 |x_1|^2 \mathbf{f}^T \mathbf{f}}\right\}, \tag{36}$$

with $\mathbf{a}$ from (5), and where τ_1 and τ_2 are the delays of the first and second arriving paths, respectively, and x_1 and x_2, are the corresponding complex propagation gains.

The approximate bias can also be expressed as a function of the first derivative of the autocorrelation function (19) evaluated at $\tau_{2,1} = \tau_2 - \tau_1$:

$$\tau_b \approx -\Re\left\{\frac{x_1^H x_2 R_s'(\tau_{2,1})}{4\pi^2 |x_1|^2 \mathbf{f}^T \mathbf{f}}\right\}. \tag{37}$$

Therefore, the bias is zero when $R_s'(\tau_{2,1}) = 0$, i.e., when the relative delay $\tau_{2,1}$ coincides with either a peak or a valley of the autocorrelation function. Note that the relative distance $c\tau_{2,1}$ corresponding to occurrences of zero bias depends only on the frequency vector $\mathbf{f}$ and is independent of the gains x_1, x_2.

The bias in (36) can be expressed as a function of the phase difference $\Delta\phi$ between x_1 and x_2. To do this, the gains are expressed in polar form as $x_i = |x_i| \exp(j\phi_i)$ for $i = 1, 2$. Then, term $x_1^H x_2$ in (36) is developed as

$$x_1^H x_2 = |x_1||x_2| \exp(j(\phi_2 - \phi_1)) = |x_1||x_2| \exp(j\Delta\phi), \tag{38}$$

where $\Delta\phi$ is the relative phase between x_1 and x_2. This yields

$$\tau_b \approx \Re\left\{\frac{j\pi |x_1||x_2| \exp(j\Delta\phi) \mathbf{f}^T \mathbf{a}\,(\tau_2 - \tau_1)}{2\pi^2 |x_1|^2 \mathbf{f}^T \mathbf{f}}\right\}. \tag{39}$$

In an L-path channel, each unconsidered reflection contributes to the total estimation bias. Therefore, the approximate bias is expressed as the sum of the biases of $L-1$ two-path channels [13], that is,

$$\tau_b \approx \sum_{l=2}^{L} \Re\left\{\frac{j\pi x_1^H x_l \mathbf{f}^T \mathbf{a}\,(\tau_l - \tau_1)}{2\pi^2 |x_1|^2 \mathbf{f}^T \mathbf{f}}\right\}. \tag{40}$$

Note that for each element of the summation in (40), the first path is the LOS path and the second is the l-th reflected path.

B. ESTIMATION BIAS VIA NUMERICAL COMPUTATION

In the second approach, the bias vector $\mathbf{b}$ is defined as the difference between the pseudotrue parameter $\boldsymbol{\theta}_0$ and true parameter $\boldsymbol{\theta}_{\text{true}}$:

$$\mathbf{b} = \boldsymbol{\theta}_0 - \boldsymbol{\theta}_{\text{true}}. \tag{41}$$

Then, the bias of the delay of the first path corresponds to the first entry of the bias vector $\mathbf{b}$, i.e., $\tau_b = [\mathbf{b}]_1$.

The pseudotrue parameter can be obtained by minimizing the KLD (31). For our problem, this translates to the minimization of [35]

$$\boldsymbol{\theta}_0 = \arg\min_{\boldsymbol{\theta}} \left\{\|\boldsymbol{\mu}(\boldsymbol{\theta}_{\text{true}}, \boldsymbol{\gamma}) - \boldsymbol{\mu}(\boldsymbol{\theta})\|^2_{\mathbf{Q}_{\mathbf{h}}^{-1}}\right\}, \tag{42}$$

where $\boldsymbol{\mu}(\boldsymbol{\theta}_{\text{true}}, \boldsymbol{\gamma})$, and $\boldsymbol{\mu}(\boldsymbol{\theta})$ are the expectations of the channel frequency response under the true distribution (30) and user-assumed distribution (29), respectively. Note that the user-assumed distribution considers less paths than in reality.

The optimization problem (42) is equivalent to the nonlinear least squares (NLS) problem with weighting matrix $\mathbf{Q}_{\mathbf{h}}^{-1}$. It can be solved using gradient decent methods [32] (e.g., Steepest Descent), the Expectation-Maximization (EM) algorithm [36], the Alternating Projection (AP) algorithm [37], the Space Alternating Generalized Expectation-Maximization (SAGE) algorithm [3], [38], as well as other iterative approaches.

The pseudotrue parameter can be expressed with (7) as

$$\boldsymbol{\theta}_0 = \left[\boldsymbol{\tau}_0^T \ \Re\{\boldsymbol{x}_0^T\} \ \Im\{\boldsymbol{x}_0^T\}\right]^T \in \mathbb{R}^{3\hat{L}\times 1}. \tag{43}$$

Contrary to the first approach (36), the number of paths in the estimation model is not limited to one, i.e., $\hat{L} \geq 1$ paths.

The minimizers of (42), can be obtained similarly to those in (10) and (12), as follows:

$$\boldsymbol{\tau}_0 = \arg\min_{\boldsymbol{\tau}} ||P^{\perp}_{A(\tau)}\boldsymbol{\mu}(\boldsymbol{\theta}_{\text{true}}, \boldsymbol{\gamma})||^2_{\mathbf{Q}_{\mathbf{h}}^{-1}},$$
$$\mathbf{x}_0 = \left(\mathbf{A}^H(\boldsymbol{\tau}_0)\mathbf{Q}_{\mathbf{h}}^{-1}\mathbf{A}(\boldsymbol{\tau}_0)\right)^{-1}\mathbf{A}^H(\boldsymbol{\tau}_0)\mathbf{Q}_{\mathbf{h}}^{-1}\boldsymbol{\mu}(\boldsymbol{\theta}_{\text{true}}, \boldsymbol{\gamma}). \quad (44)$$

We denote the pseudotrue delays with subscript $\boldsymbol{\tau}_0$, following the same notation in [6]; note that this is unrelated to the first arriving path of the channel.

Similarly to (9) and (10), the minimizers can only be obtained when $\mathbf{A}(\boldsymbol{\tau}_0)$ is full column rank, requiring the path delays $\boldsymbol{\tau}_0$ to be non-degenerative. In practice, evaluating bias and variance for very closely spaced paths is not meaningful, since, as we have shown in Fig. 1, the estimator's variance tends to infinity.

Then, the TDE bias of the first arriving path using an MS-unbiased estimator is defined as

$$\tau_b = [\boldsymbol{\tau}_0 - \boldsymbol{\tau}_{\text{true}}]_1, \quad (45)$$

where $\boldsymbol{\tau}_{\text{true}}$ is the true parameter vector containing the path delays.

Note that, contrary to the analytical expression in (40), the bias defined in (45) is obtained via numerical optimization of (44). Additionally, expressions for the bias using the first approach (36), (39) and (40) are only applicable when the user considers a single-path model $\hat{L} = 1$, while the second approach allows for a generic estimation model with $\hat{L} \geq 1$ paths.

C. MULTIPATH ERROR ENVELOPE

The maximum bias occurs when the multipath arrives either in-phase ($\Delta\phi = 0$ rad) or out-of-phase ($\Delta\phi = \pi$ rad) with respect to the LOS path. This maximum bias, referred to as multipath error envelope (MPEE), is a metric to evaluate the TDE bias due to an unconsidered multipath component [39], [40]. In this paper, we use the MPEE to qualitatively show the estimation bias as a function of delay separation for different relative carrier phases between the first and second path.

Figure 2 shows the bias of the time-delay estimator of the first path in a two-path channel. In this setup, the receiver estimates delay $\hat{\tau}_1$ and gain $\hat{x}_1$ of the first path but does not account for the reflection (solid and black dashed curves). In addition, the yellow dashed curve shows the bias obtained for $\Delta\phi = \pi/2$, when the receiver estimates only the delay, assuming the gain x_1 of the first path is known. The bias is computed for an OFDM signal and a channel using the parameters listed in Table 1. The gains are set to $x_1 = 1$, and $x_2 = 0.7\exp(j\Delta\phi)$, where $\Delta\phi$ is the carrier phase difference between the paths. The dashed curves represent the bias obtained for different values of carrier phase difference $\Delta\phi$.

We clearly see that the bias is bounded by the constructive and destructive multipath components (blue and red curves, respectively). For $\Delta\phi = \pi/2$ (in yellow), the bias is approximately zero when the relative distance between the paths is greater than $c/B = 1.87$ m, where B is the signal bandwidth and c is the speed of light. When the gain is assumed known, the bias for $\Delta\phi = \pi/2$ is zero for all relative distances. Moreover, for $\Delta\phi = 0$ and $\Delta\phi = \pi$, the bias is identical whether the gain is estimated or assumed known (plots not shown for ease of interpretation).

VII. MISSPECIFIED CRB

In Section V, we introduced two models: the misspecified model $\mathcal{F}_{\hat{L}}$ (33) that considers less paths than actually present in the measured channel frequency response, and the true model $\mathcal{G}_L$ (34), which considers all the paths. After that, in Section VI we derived the bias in the time-delay estimator of the first arriving path when the misspecified model was used.

In this section, we derive a bound on the variance $\sigma^2_{\hat{\tau}_1}$ of the time-delay estimator $\hat{\tau}_1$ of the first path when the misspecified model is used ($\hat{L} < L$), based on the MCRB. From now on, we focus on the MML estimator $\hat{\boldsymbol{\theta}}_{\text{MML}}$ (32).

The aim is to bound the variance of $\hat{\boldsymbol{\theta}}_{\text{MML}}$, which is equivalent to bounding the zero-mean estimation error defined as

$$\underline{\boldsymbol{\zeta}} = \hat{\underline{\boldsymbol{\theta}}}_{\text{MML}} - \mathbb{E}_g\{\hat{\underline{\boldsymbol{\theta}}}_{\text{MML}}\} = \hat{\underline{\boldsymbol{\theta}}}_{\text{MML}} - \boldsymbol{\theta}_0, \quad (46)$$

where $\mathbb{E}_g\{\hat{\underline{\boldsymbol{\theta}}}_{\text{MML}}\} = \boldsymbol{\theta}_0$ for high SNR values (32).

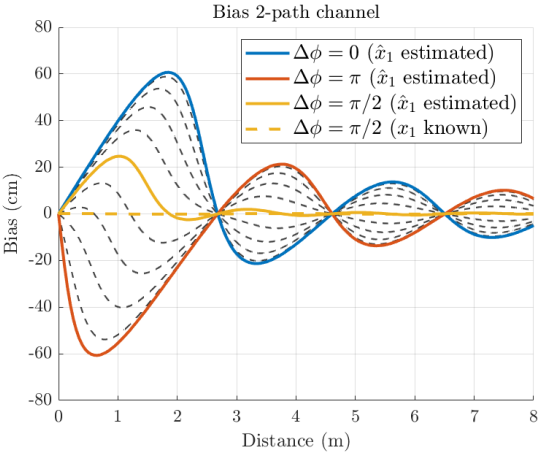

FIGURE 2. Bias of the time-delay estimator $\hat{\tau}_1$ of the first path ($\hat{L} = 1$) in a two-path channel ($L = 2$) as a function of the path separation $c\tau_{21}$ as a distance. Solid curves and dashed black curves corresponds to a receiver that estimates only the delay $\hat{\tau}_1$ and gain $\hat{x}_1$ of the first path and neglects the multipath component. Dashed black curves represent the bias obtained for different values of carrier phase difference $\Delta\phi \in [0, 2\pi]$. The dashed yellow curve corresponds to a receiver that has knowledge of the first-path gain x_1 and estimates only its delay while neglecting the multipath component. OFDM parameters are shown in table 1.

The covariance of the error vector $\underline{\boldsymbol{\zeta}}$ can be lower bounded using the Cauchy-Schwarz inequality [5]. In its multivariate form, this covariance inequality is given by

$$\mathbb{E}_g\left[\underline{\boldsymbol{\zeta}}\underline{\boldsymbol{\zeta}}^H\right] \geq \mathbb{E}_g\left[\underline{\boldsymbol{\zeta}}\underline{\boldsymbol{\eta}}^H\right]\left(\mathbb{E}_g\left[\underline{\boldsymbol{\eta}}\underline{\boldsymbol{\eta}}^H\right]\right)^{-1}\mathbb{E}_g[\underline{\boldsymbol{\eta}}\underline{\boldsymbol{\zeta}}^H], \quad (47)$$

where $\underline{\boldsymbol{\eta}}$ denotes the *score function*.

In general, the bound (47) is applicable to any choice of score function $\underline{\boldsymbol{\eta}}$, however, a tighter bound is obtained if the score function is defined by

$$\underline{\boldsymbol{\eta}} = \frac{\partial \ln f_{\underline{\mathbf{h}}}(\underline{\mathbf{h}}|\boldsymbol{\theta})}{\partial \boldsymbol{\theta}} - \mathbb{E}_g\left\{\frac{\partial \ln f_{\underline{\mathbf{h}}}(\underline{\mathbf{h}}|\boldsymbol{\theta})}{\partial \boldsymbol{\theta}}\right\}. \tag{48}$$

By expanding the terms of the covariance inequality (47), a general expression for the MCRB can be derived following Appendix I of [5], and then particularizing for the case of a variance matrix $\mathbf{Q_h} = \sigma_n^2 \mathbf{I}_{N_s}$. Accordingly, the MCRB on the variance of an MS-unbiased estimator which considers less paths than in reality ($\hat{L} < L$) is given by:

$$\begin{aligned}&\mathbb{E}_g\{(\hat{\underline{\boldsymbol{\theta}}}_{\text{MML}} - \boldsymbol{\theta}_0)(\hat{\underline{\boldsymbol{\theta}}}_{\text{MML}} - \boldsymbol{\theta}_0)^T\}\\ &\geq \mathbf{C}^{-1}(\boldsymbol{\theta}_0)\,\mathbf{FIM}(\boldsymbol{\theta}_0)\,\mathbf{C}^{-1}(\boldsymbol{\theta}_0)\\ &= \mathbf{MCRB}(\boldsymbol{\theta}_0)\end{aligned} \tag{49}$$

where

$$\begin{aligned}\mathbf{C}(\boldsymbol{\theta}_0) &= \mathbf{D}(\boldsymbol{\theta}_0) - \mathbf{FIM}(\boldsymbol{\theta}_0),\\ [\mathbf{D}(\boldsymbol{\theta}_0)]_{i,k} &= \frac{2}{\sigma_n^2}\Re\left[\left(\frac{\partial^2 \boldsymbol{\mu}(\boldsymbol{\theta}_0)}{\partial\theta_i \partial\theta_k}\right)^H \Delta\boldsymbol{\mu}(\boldsymbol{\theta}_0)\right],\\ \mathbf{FIM}(\boldsymbol{\theta}_0) &= \frac{2}{\sigma_n^2}\Re\left[\left(\frac{\partial \boldsymbol{\mu}(\boldsymbol{\theta}_0)}{\partial \boldsymbol{\theta}^T}\right)^H \frac{\partial \boldsymbol{\mu}(\boldsymbol{\theta}_0)}{\partial \boldsymbol{\theta}^T}\right],\\ \Delta\boldsymbol{\mu}(\boldsymbol{\theta}_0) &= \left(\sum_{i=1}^{L} x_i \mathbf{a}(\tau_i)\right) - \mathbf{A}(\boldsymbol{\tau}_0)\boldsymbol{x}_0,\end{aligned} \tag{50}$$

and $\boldsymbol{\theta}_0$ is the pseudotrue parameter (31), $\boldsymbol{\tau}_0$ and $\boldsymbol{x}_0$ are the pseudotrue vectors of delays and complex gains, and τ_i and x_i (for $i = 1, \cdots, L$) are the true delay and complex gain of the i-th path in the channel frequency response. The term $\Delta\boldsymbol{\mu}(\boldsymbol{\theta}_0)$ is the difference between the expectation of the true and assumed models. If one is only interested in lower bounding the variance of the TDE of the first path, then entry $(1, 1)$ of the right-hand side of (49) is used. The MCRB in (49) and (50) is applicable whether the path gains are jointly estimated with the delay or assumed known.

The dimensions of the matrices in (49) and (50) are given by $\mathbf{C}(\boldsymbol{\theta}_0) \in \mathbb{R}^{3\hat{L}\times 3\hat{L}}$ and $\mathbf{D}(\boldsymbol{\theta}_0) \in \mathbb{R}^{3\hat{L}\times 3\hat{L}}$. The indices in $[\mathbf{D}(\boldsymbol{\theta}_0)]_{i,k}$, take the values $i = 1, \cdots, 3\hat{L}$ and $k = 1, \cdots, 3\hat{L}$.

Matrix $\mathbf{FIM}(\boldsymbol{\theta}_0)$ in (49) and (50) is equivalent to the general expression of the Fisher information matrix in (15) evaluated at $\boldsymbol{\theta}_0$.

Note that computing the MCRB involves the evaluation of $\mathbf{D}(\boldsymbol{\theta}_0)$ and $\mathbf{FIM}(\boldsymbol{\theta}_0)$ at the pseudotrue parameter $\boldsymbol{\theta}_0$. This parameter can be obtained by optimizing (42) and (44). In this section, we assume that the user's time-delay estimation model includes $\hat{L}$ paths, which is fewer than the actual number of paths L present in the channel. Therefore, the pseudotrue parameter is composed of $3\hat{L}$ terms (43).

Matrix $\mathbf{D}(\boldsymbol{\theta}_0)$ in (50) requires the computation of the Hessian of $\boldsymbol{\mu}(\boldsymbol{\theta}_0)$, which is obtained from the second-order derivatives provided in (69) in Appendix B. Accordingly, $\mathbf{D}(\boldsymbol{\theta}_0)$ can be expressed as

$$\mathbf{D}(\boldsymbol{\theta}_0) = \frac{2}{\sigma_n^2}\begin{bmatrix}\mathbf{D}_{\boldsymbol{\tau}} & \mathbf{D}_{\boldsymbol{\tau}\mathbf{x}}\\ \mathbf{D}_{\mathbf{x}\boldsymbol{\tau}} & \mathbf{D}_{\mathbf{x}}\end{bmatrix}, \tag{51}$$

where

$$\begin{aligned}\mathbf{D}_{\boldsymbol{\tau}} &= -4\pi^2\Re\{\text{diag}(\mathbf{x}_0^*)\,\text{diag}(\mathbf{A}_0^H(\mathbf{f}\odot\mathbf{f}\odot\Delta\boldsymbol{\mu}(\boldsymbol{\theta}_0)))\},\\ \mathbf{D}_{\mathbf{x}} &= \mathbf{0}_{2\hat{L}\times 2\hat{L}},\\ \mathbf{D}_{\mathbf{x}\boldsymbol{\tau}} &= \mathbf{D}_{\boldsymbol{\tau}\mathbf{x}}^T = 2\pi\begin{bmatrix}-\Im\{\text{diag}(\mathbf{A}_0^H(\mathbf{f}\odot\Delta\boldsymbol{\mu}(\boldsymbol{\theta}_0)))\}\\ \Re\{\text{diag}(\mathbf{A}_0^H(\mathbf{f}\odot\Delta\boldsymbol{\mu}(\boldsymbol{\theta}_0)))\}\end{bmatrix},\end{aligned} \tag{52}$$

where $\mathbf{A}_0$ is the matrix in (5) evaluated at the pseudotrue delays, i.e., $\mathbf{A}_0 = \mathbf{A}(\boldsymbol{\tau}_0)$.

The MCRB is guaranteed to exist if the user-assumed model $\mathcal{F}_{\hat{L}}$ (33) is regular with respect to the true model $\mathcal{G}_L$ (34). This requires the pseudotrue parameter $\boldsymbol{\theta}_0$ to exist, be unique, and lie in an interior point of $\boldsymbol{\Theta}$. In the OFDM ranging problem, this condition translates into the solvability of (44), which in turn requires $\mathbf{A}(\boldsymbol{\tau}_0)$ to be full column rank and the path delays $\boldsymbol{\tau}_0$ to be non-degenerate. Furthermore, matrix $\mathbf{C}(\boldsymbol{\theta}_0)$ must be nonsingular. As shown in [24], additional regularity conditions related to the twice differentiability of the mean of the user-assumed PDF are also required. In Appendix B we show that, for the OFDM ranging model, the mean of the PDF is twice differentiable.

A. MCRB FOR 1-PATH ESTIMATOR IN L-PATH CHANNEL

This section derives a semi-closed form expression for a lower bound on the variance of the first path's time-delay estimator. Specifically, the derivation addresses a model mismatch where the user assumes a single path $\hat{L} = 1$, but the channel contains a LOS component and $L - 1$ reflected multipath components. For this case, we consider a receiver that only estimates the time-delay of the first path, not the gain, i.e., the user assumed expectation of the channel frequency response is $\boldsymbol{\mu}(\theta) = x_1\mathbf{a}(\tau_1)$, with gain x_1 known. The derivation is based on the general MCRB expression given in (49). By expanding the terms in (49), the MCRB is expressed as

$$\boxed{\sigma^2_{\text{MCRB}} = \frac{\sigma^2_{\text{CRB}}}{\left(\frac{1}{|x_1|^2}\Re\left\{x_1^H\sum_{i=1}^{L} x_i\mathbf{a}^T(\tau_i - \tau_0)\right\}\frac{\mathbf{f}\odot\mathbf{f}}{\mathbf{f}^T\mathbf{f}}\right)^2}} \tag{53}$$

where σ^2_{CRB} is the CRB for the single-path AWGN channel (17). The terms $x_1, \cdots, x_L$ and $\tau_1, \cdots, \tau_L$ are the complex gains and delays, respectively, of the L paths present in the channel frequency response, and τ_0 is the pseudotrue delay obtained with (42), where $\boldsymbol{\mu}(\boldsymbol{\theta}_{\text{true}}, \boldsymbol{\gamma}) = \sum_{i=1}^{L} x_i\mathbf{a}(\tau_i)$. Note that, for a single-path channel ($L = 1$) the denominator in (53) equals one, so that the MCRB reduces to the single-path CRB.

The variance of the time-delay estimator of the first path in a two-path channel can be expressed as a function of the second derivative of the signal ACF (19) evaluated at $\tau = 0$, i.e., $R_s''(0)$ in (70), and the real part of the second

derivative of the cross-correlation function evaluated at the pseudotrue delay τ_0, i.e., $\Re\left\{R''_{\boldsymbol{\mu},\mathbf{d}}(\tau_0)\right\}$ in (70):

$$\sigma^2_{\text{MCRB}} = \frac{\sigma_n^2|x_1|^2 R''_s(0)}{-2\Re\{R''_{\boldsymbol{\mu},\mathbf{d}}(\tau_0)\}^2} \propto \frac{R''_s(0)}{-\Re\{R''_{\boldsymbol{\mu},\mathbf{d}}(\tau_0)\}^2}, \tag{54}$$

where the cross-correlation function between the parameterized expectation of the user-assumed CFR (29), i.e., the single-path template $\boldsymbol{\mu} = x_1\mathbf{a}(\tau)$ with known gain x_1, and the expectation of the true CFR under a two-path channel, i.e., $\mathbf{d} = x_1\mathbf{a}(\tau_1) + x_2\mathbf{a}(\tau_2)$, is defined as

$$R_{\boldsymbol{\mu},\mathbf{d}}(\tau) = (x_1\mathbf{a}(\tau))^H(x_1\mathbf{a}(\tau_1) + x_2\mathbf{a}(\tau_2)). \tag{55}$$

Its first- and second-order derivatives are derived in Appendix C.

The MCRB is proportional to the ratio of the curvature of the ACF at the mainlobe and the square of the real part of the cross-correlation curvature evaluated at the pseudotrue delay. The numerator in (54) depends only on the signal bandwidth, whereas the denominator captures the interaction between the first path and the multipath component through the cross-correlation term. Since this curvature appears squared, any curvature reduction caused by multipath results in an increase of the MCRB (worse precision). Conversely, a larger cross-correlation curvature reduces the MCRB and improves the achievable estimation precision.

The MCRB in (53), can also be expressed as a function of the relative carrier between the first arriving path and the other $L-1$ paths as

$$\sigma^2_{\text{MCRB}} = \frac{\sigma^2_{\text{CRB}}}{\left(\frac{1}{|x_1|}\Re\left\{\sum_{i=1}^{L}|x_i|\exp(j\Delta\phi_{i,1})\mathbf{a}^T(\tau_i-\tau_0)\right\}\frac{\mathbf{f}\odot\mathbf{f}}{\mathbf{f}^T\mathbf{f}}\right)^2}, \tag{56}$$

where $\Delta\phi_{i,1} = \phi_i - \phi_1$ is the carrier phase difference between the i-th path and the first arriving path. Expression (56) is obtained by using the polar form of the complex propagation gains x_i, as in (23).

As to analyse a limiting case, let us now derive the MCRB for the first path estimator ($\hat{L} = 1$) in a two-path channel ($L = 2$) when both paths arrive at the same time, i.e., $\tau_1 = \tau_2$. We assume that gain x_1 is known as in (53). In this scenario, the pseudotrue parameter τ_0 is equal to τ_1, since the TDE bias is zero (similar to Fig. 2 when distance $c\tau_{21} = 0$). Under these conditions the MCRB (53) becomes

$$\sigma^2_{\text{MCRB}}\Big|_{L=2;\tau_1=\tau_2=\tau_0} = \frac{\sigma^2_{\text{CRB}}}{\left(\frac{1}{|x_1|^2}\Re\left\{x_1^H x_1 + x_1^H x_2\right\}\right)^2}. \tag{57}$$

Expressing the MCRB in terms of the amplitude ratio $|x_2|/|x_1|$ and the relative carrier phase $\Delta\phi = \phi_2 - \phi_1$ between the paths yields a more intuitive form:

$$\sigma^2_{\text{MCRB}}\Big|_{L=2;\tau_1=\tau_2=\tau_0} = \frac{\sigma^2_{\text{CRB}}}{\left(1 + \frac{|x_2|}{|x_1|}\cos(\Delta\phi)\right)^2}. \tag{58}$$

For a constructive multipath component ($\Delta\phi = 0$), the MCRB in (58) is minimized; for destructive multipath ($\Delta\phi = \pi$), the MCRB is maximized; and for a carrier phase shift of $\Delta\phi = \pi/2$, the multipath component has no effect, and the MCRB reduces to the CRB for the single-path channel σ^2_{CRB}. This behavior is illustrated in Fig 3.

Figure 3 shows the MCRB of the time-delay estimator of the first path obtained with (53) for a two-path channel ($L = 2$) with gains $x_1 = 1$, and $x_2 = 0.7\exp(j\Delta\phi)$, where $\Delta\phi$ is the relative carrier phase between both paths. The MCRB is shown as a function of the relative distance between the paths. The results are obtained for an OFDM signal with parameters as indicated in Table 1, which is the same configuration as in Fig. 1 and Fig. 2. We observe that for a relative carrier phase of $\Delta\phi = \pi/2$ (yellow curve in Fig. 3), the MCRB remains constant across all relative distances. This constant value of 0.72 cm matches the CRB of the single-path MLE (17). Hence, for $\Delta\phi = \pi/2$ the variance of the TDE for the first path is unaffected by the second path.

The blue and red curves in Fig. 3 represent the MCRB for a constructive and destructive reflection, respectively. In general, constructive and destructive multipath define the lower and upper bounds of the estimation variance. Which one forms the lower or upper bound depends on the relative path distance, and this role alternates as the path separation varies. An exception of this trend occurs around 1.2, 3.5, 5.5 and 7.4 m, which coincide with the zero-crossings of the second derivative of the bandlimited signal's autocorrelation function. Note that in Fig. 3, multipath does not always degrade the precision of the time-delay estimator. For certain path separations and relative carrier phases $\Delta\phi$, the variance indicated by the MCRB (53) can be equal or even lower than the CRB (17). This occurs because the multipath component can constructively interfere with the LOS path, producing an overall channel impulse response with a higher main peak amplitude than the LOS alone.

Figure 4 shows the MCRB for a receiver that jointly estimates the delay and gain of the first arriving path while ignoring the multipath component. This corresponds to the same scenario as in Fig. 3, except that the gain is also included in the estimation. We observe that the MCRB for a constructive ($\Delta\phi = 0$) and a destructive ($\Delta\phi = \pi$) multipath component, remains the same as in Fig. 3. However, for intermediate values of relative carrier phase $\Delta\phi$ the MCRB is different. In particular, the MCRB increases considerably for $\Delta\phi = \pi/2$, and distance $c\tau_{21}$ between 1 and 2 m. This behaviour occurs for closely spaced multipath components, where the receiver finds it difficult to resolve the first path.

B. MCRB AND CROSS-CORRELATION FUNCTION

In the following we provide a qualitative description of the behaviour of the MCRB in Fig. 3, which shows the variance of an estimator that assumes a single-path channel ($\hat{L} = 1$) with only delay estimation of the first path assuming the gain x_1 is known, whereas the actual channel contains $L = 2$ paths.

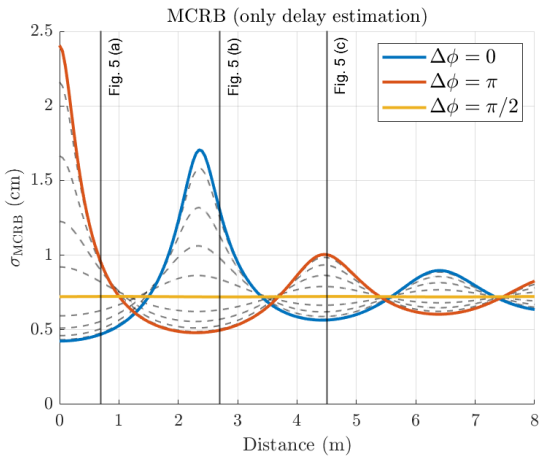

FIGURE 3. Square root of the MCRB of the time-delay estimator of the first path ($\hat{L} = 1$) in a two-path channel ($L = 2$) as a function of the path separation $c\tau_{21}$. The receiver estimates only the delay of the first path with known gain and neglects the multipath component. OFDM parameters are shown in table 1. Dashed black curves represent the MCRB obtained for different values of carrier phase difference $\Delta\phi \in [0, 2\pi]$. The standard deviation indicated by the CRB is $\sigma_{\text{CRB}} = 0.72$ cm, and coincides with the yellow line. Each vertical line corresponds to a specific case depicted in fig. 5.

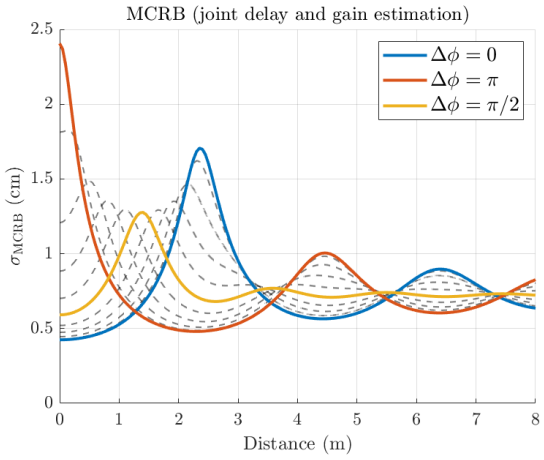

FIGURE 4. Square root of the MCRB of the time-delay estimator of the first path ($\hat{L} = 1$) in a two-path channel ($L = 2$), as a function of the path separation $c\tau_{21}$. The receiver jointly estimates the delay and the gain of the first path and neglects the multipath component. OFDM parameters are shown in table 1. Dashed black curves represent the MCRB obtained for different values of carrier phase difference $\Delta\phi \in [0, 2\pi]$.

Here, $\boldsymbol{\mu} = x_1\mathbf{a}(\tau)$ represents the parameterized mean of the user-assumed distribution of the CFR, under the assumption that the first-path gain x_1 is known and that the estimator adopts a single-path model. The true mean of the CFR is given by $\mathbf{d} = x_1\mathbf{a}(\tau_1) + x_2\mathbf{a}(\tau_2)$, which consists of two propagation paths. We further define the individual path contributions as $\mathbf{d}_1 = x_1\mathbf{a}(\tau_1)$ and $\mathbf{d}_2 = x_2\mathbf{a}(\tau_2)$.

Then, we decompose the cross-correlation function (55) between $\boldsymbol{\mu}$ and $\mathbf{d}$ by

$$R_{\boldsymbol{\mu},\mathbf{d}}(\tau) = R_{\boldsymbol{\mu},\mathbf{d}_1}(\tau) + R_{\boldsymbol{\mu},\mathbf{d}_2}(\tau), \tag{59}$$

where $R_{\boldsymbol{\mu},\mathbf{d}_i}(\tau) = (x_1\mathbf{a}(\tau))^H(x_i\mathbf{a}(\tau_i))$ for $i = 1, 2$ represent the cross-correlations between the user-assumed mean and the first and second path components of the true mean, respectively.

Figure 5 illustrates the individual cross-correlation functions $R_{\boldsymbol{\mu},\mathbf{d}_1}(\tau)$ and $R_{\boldsymbol{\mu},\mathbf{d}_2}(\tau)$ of each path in a two-path channel ($L = 2$) and the total cross-correlation function $R_{\boldsymbol{\mu},\mathbf{d}}(\tau)$ (light blue dashed curve), demonstrating how the carrier phase difference $\Delta\phi$ between both paths impacts estimation performance. We show the real part of the cross-correlations for illustration purposes since the gain x_1 is real-valued. Moreover, because the spectrum is slightly asymmetric around subcarrier 0 (by one subcarrier), the imaginary part is significantly smaller than the real component; therefore, we focus on the real part. This asymmetry is commonly encountered in OFDM systems, where the subcarrier indices typically range from $-N_s/2$ to $N_s/2 - 1$.

The total cross-correlation function $R_{\boldsymbol{\mu},\mathbf{d}}(\tau)$ in Fig. 5 (a) for a path separation of $c\tau_{2,1} = 0.7$ m reveals that a constructive reflection ($\Delta\phi = 0$) increases the main peak's amplitude, thereby increasing the effective SNR and thus improving estimation precision, as shown in expression (17). Conversely, a destructive reflection ($\Delta\phi = \pi$) reduces the main peak amplitude of $R_{\boldsymbol{\mu},\mathbf{d}}(\tau)$, degrading precision. For a reflection with carrier phase difference $\Delta\phi = \pi/2$, the main peak amplitude of the cross-correlation function $R_{\boldsymbol{\mu},\mathbf{d}}(\tau)$ is the same to the one of the LOS case $R_{\boldsymbol{\mu},\mathbf{d}_1}(\tau)$, indicating the same precision. This aligns with the precision indicated by the MCRB in Fig. 3, confirming that for a path separation of $c\tau_{21} = 0.7$ m, precision is improved, worsened, or remains unchanged for $\Delta\phi = 0$, $\Delta\phi = \pi$, and $\Delta\phi = \pi/2$, respectively.

Furthermore, the estimation bias is different in each scenario. As shown in Fig. 5 (a), the main peak of the total cross-correlation is displaced by 28.4 cm (positive bias) for $\Delta\phi = 0$, and -60.5 cm (negative bias) for $\Delta\phi = \pi$. In contrast, for $\Delta\phi = \pi/2$ it is not displaced. The displacements observed for these values of $\Delta\phi$ in Fig. 5 are consistent with the bias shown in Fig. 2 at a relative distance of $c\tau_{21} = 0.7$ m.

Figures 5 (b) and (c) show the individual cross-correlation functions and their combined result when the second path arrives at a relative distance from the LOS path of $c\tau_{2,1} = 2.7$ m and of $c\tau_{2,1} = 4.5$ m, respectively. In (b), the precision of the time-delay estimator degrades in the presence of a constructive reflection ($\Delta\phi = 0$). This occurs because the main peak of the LOS contribution overlaps with a negative sidelobe of the multipath component, reducing the amplitude of the resulting peak. The opposite behaviour is observed for a multipath component with $\Delta\phi = \pi$, where the sidelobe has positive magnitude, leading to an increase in amplitude of the main cross-correlation peak. In (c), for both $\Delta\phi = 0$ and $\Delta\phi = \pi$, the main LOS peak aligns with the second secondary peak of the multipath component; however, the resulting amplitude of the cross-correlation differs in each case due to the different phase relationships.

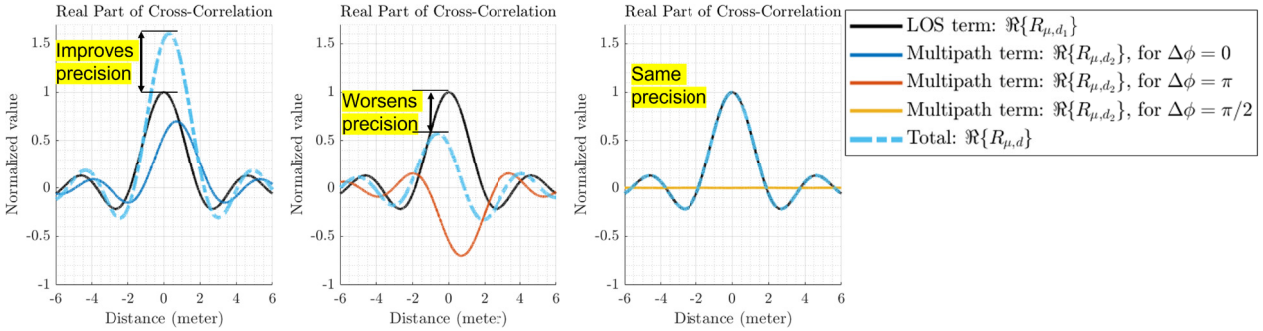

(a) Relative distance between the first and second paths is 0.7 m.

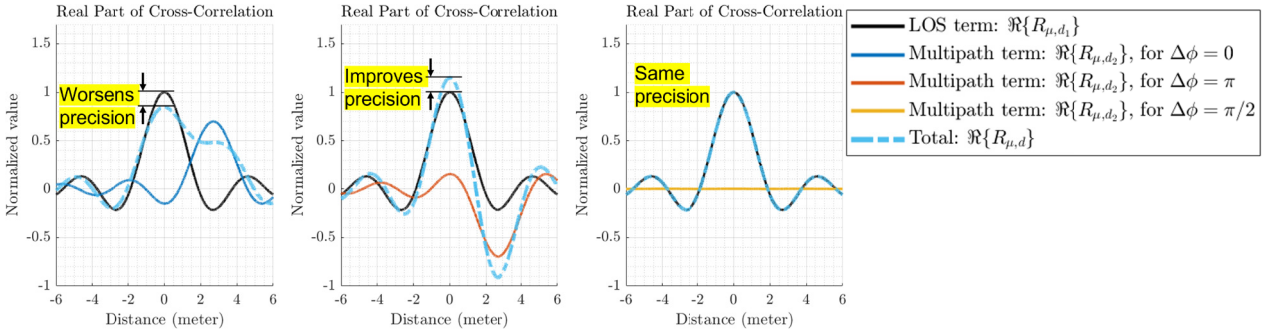

(b) Relative distance between the first and second paths is 2.7 m.

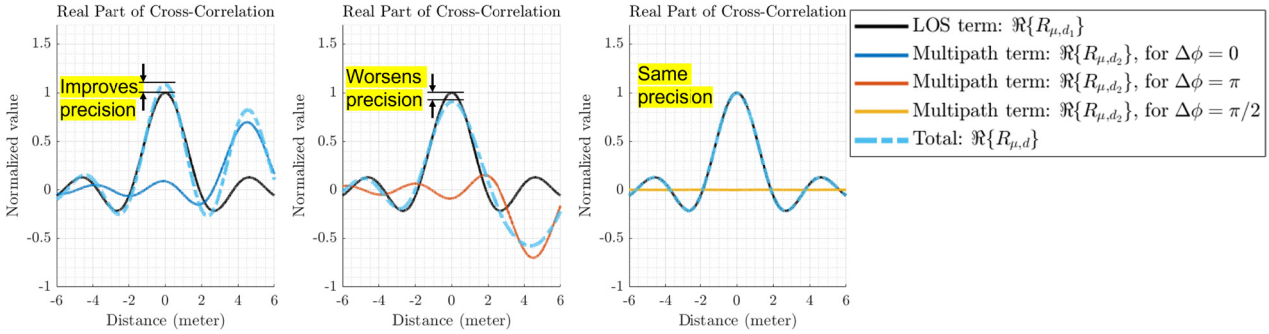

(c) Relative distance between the first and second paths is 4.5 m.

FIGURE 5. Real part of the cross-correlation functions versus delay (in distance units) for parameters in table 1. The cross-correlations are normalized with respect to the cross-correlation of the first arriving path $R_{\mu,\mathbf{d}_1}(\tau)$ in (59). Individual cross-correlations are shown as solid curves: the LOS path (black), constructive and destructive multipath (blue and red, respectively), and a multipath component with a relative carrier phase of $\Delta\phi = \pi/2$ (yellow). From left to right, the light blue dashed curve shows the resulting cross-correlation from the superposition of the LOS path with the constructive, destructive, and a multipath component with $\Delta\phi = \pi/2$, respectively. From top to bottom, each row corresponds to a scenario where the multipath component arrives at a relative distance of 0.7 m, 2.7 m, and 4.5 m, respectively.

VIII. BOUND ON MSE

When all the paths present in the channel frequency response are jointly estimated, the estimator is unbiased and the CRBs of Section IV bound the estimation precision and the MSE.

In the case of model order mismatch, in which the receiver employs an under-parameterized estimation model, i.e., it assumes fewer paths than present in the actual channel ($\hat{L} < L$), the MSE bound is obtained by decomposing it into the variance plus the square of the bias. This is possible, thanks to the nested structure of the user-assumed model (33) into the true model (34), [6]. For an under-parameterized estimation model, the MSE matrix can be bounded as

$$\begin{aligned}\mathbf{MSE}(\boldsymbol{\theta}_0) &= \mathbb{E}_g\{(\hat{\underline{\boldsymbol{\theta}}}_{\mathrm{MML}} - \boldsymbol{\theta}_{\mathrm{true}})(\hat{\underline{\boldsymbol{\theta}}}_{\mathrm{MML}} - \boldsymbol{\theta}_{\mathrm{true}})^T\} \\ &\geq \mathbf{MCRB}(\boldsymbol{\theta}_0) + \mathbf{b}\mathbf{b}^T, \end{aligned} \tag{60}$$

where $\mathbf{MCRB}(\boldsymbol{\theta}_0)$ is the misspecified Cramér-Rao bound (49), and $\mathbf{b}$ is the bias vector (41).

From the bound on the MSE matrix (60) one can obtain a bound on the TDE of the first arriving path by taking element (1, 1) of matrix $\mathbf{MSE}(\boldsymbol{\theta}_0)$ evaluated at the pseudotrue parameter $\boldsymbol{\theta}_0$ (31).

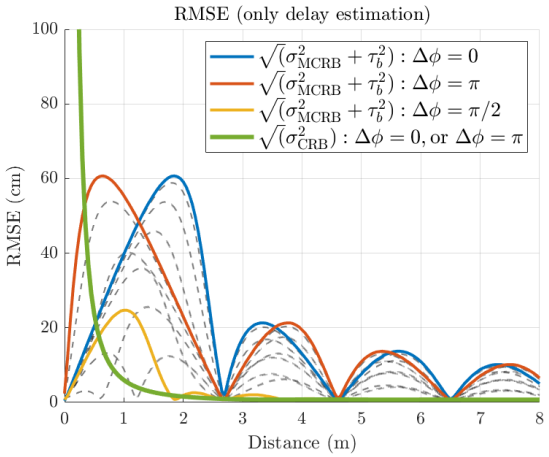

FIGURE 6. RMSE of the time-delay estimator of the first path in a two-path channel as a function of the path separation $c\tau_{21}$ (distance). Blue, red, and yellow curves correspond to a receiver that jointly estimates the delay and gain of the first path and neglects the multipath component ($\hat{L} = 1, L = 2$). The green curve corresponds to the 2-path MLE that jointly estimates delay and gain of both paths ($\hat{L} = 2, L = 2$). OFDM parameters are shown in table 1, and SNR = 10dB. Dashed black curves represent the RMSE obtained for different values of carrier phase difference $\Delta\phi \in [0, 2\pi]$.

TABLE 2. How to compute bias and variance bound based on the number of paths in the channel L and MLE model order $\hat{L}$. In the second and fourth row ($\hat{L} = 1$), the variance of the first-path time-delay estimator follows from (53) when the path gains are known, and from the general expressions (49) and (50) when the delays and gains are jointly estimated.

# Paths	# Paths MLE	Bias	Variance
1	1	0	CRB (17)
2	1	Minimize KLD (41), (42)	MCRB (53), (49), (50)
	2	0	CRB (27)
3	1	Minimize KLD (41), (42)	MCRB (53), (49), (50)
	2	Minimize KLD (41), (42)	MCRB (49), (50)
	3	0	CRB (14), (20), (21)
L	$\hat{L} \leq L$	Minimize KLD (41), (42)	MCRB (49), (50)
	L	0	CRB (14), (20), (21)

Table 2 summarizes how to compute the bias and variance when the estimation model order matches the number of paths in the channel (white cells, $\hat{L} = L$), and when using an under-parameterized estimation model (blue cells, $\hat{L} < L$). The first column indicates the actual number of paths L in the channel frequency response, and the second column refers to the number of paths accounted for in the TDE model $\hat{L}$ (4). The numbers in brackets in the table refer to applicable equations.

Figure 6 shows the square root of the MSE bound on the time-delay estimator of the first path as a function of the relative distance between the first and second arriving paths. Blue, red and yellow curves correspond to the scenario that assumes joint delay and gain estimation of the first path (single-path MLE, $\hat{L} = 1$), while the green curve considers joint delay and gain estimation of both paths (2-paths MLE, $\hat{L} = 2$). For the latter case (green curve), we plot the square root of the CRB for constructive and destructive multipath because it yields the worse estimation precision across all values of $\Delta\phi$ (see Fig. 1). The results are obtained for an OFDM signal propagating through a two-path channel using the parameters in Table 1. For relative distances larger than the delay resolution $c/B = 1.87$ m, we observe that a reflection with a carrier phase difference of $\Delta\phi = \pi/2$ has little impact on the accuracy of the time-delay estimator of the first arriving path.

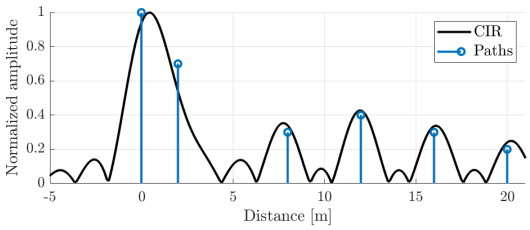

FIGURE 7. Simulated channel impulse response with six paths ($L = 6$). The path separations with respect to the first arriving path are $c\tau_{l1} = [0, 2, 8, 12, 16, 20]$ m, and the path gains are $\mathbf{x} = [1, 0.7, 0.3, 0.4, 0.3, 0.2]$.

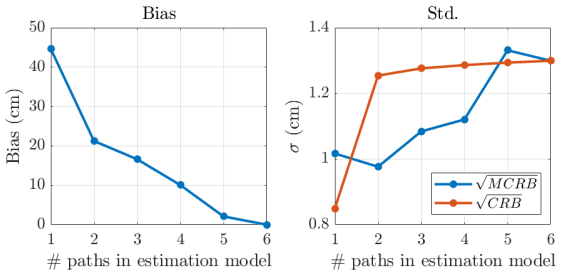

FIGURE 8. Bias of the first arriving path estimator (left) and the corresponding MCRB (in blue) and CRB (in red) (right) as functions of the number of paths considered in the estimation model $\hat{L}$ for the CIR shown in fig. 7 ($L = 6$). OFDM parameters are listed in table 1.

From a practical perspective, these results indicate that for very small path separations, the 1-path MLE is preferable, as the variance of the 2-path MLE becomes significantly larger than the RMSE obtained with the 1-path MLE. This has direct implications for receiver design, since applying a higher-order model is not always beneficial in very closely spaced multipath conditions. For the example shown in Fig. 6, corresponding to an SNR of 10 dB, the 2-path MLE only outperforms the 1-path MLE when the path separation exceeds $c\tau_{2,1} > 52.6$ cm for a multipath component of $\Delta\phi = 0$, and $c\tau_{2,1} > 33.7$ cm for $\Delta\phi = \pi$. For smaller path separations, the increase in variance of the 2-path estimator is more significant than the reduction in bias, which leads to worse overall performance. At lower SNR values, the

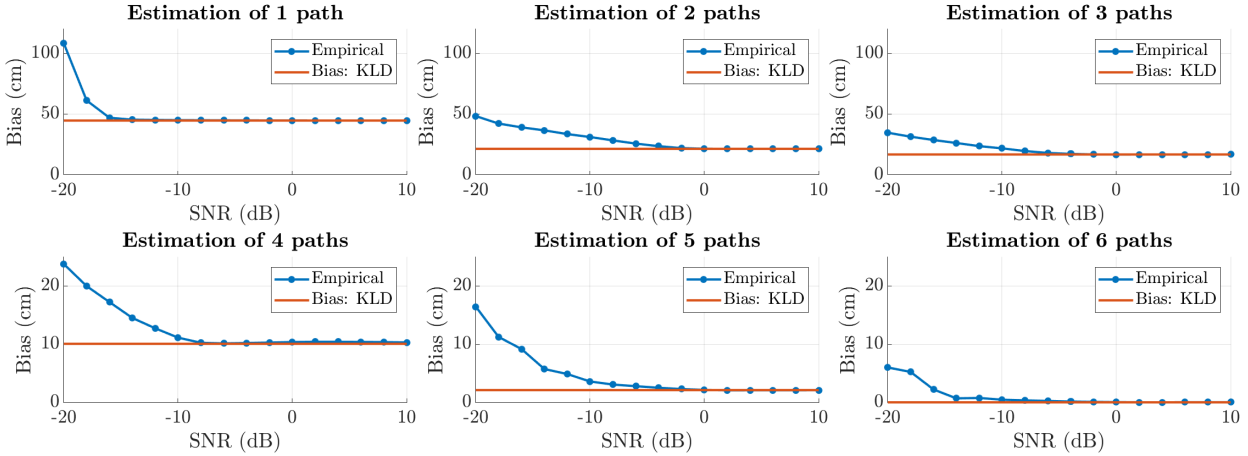

FIGURE 9. Mean error of the estimated delay of the first arriving path for the $L = 6$ paths channel impulse response shown in fig. 7 as a function of SNR. The empirical results are obtained using the steepest descent method over 2000 realizations (blue) and the bias is computed by minimizing the Kullback-Leibler divergence (41), (42) (red). Each subplot corresponds to a different number of jointly estimated paths $\hat{L}$.

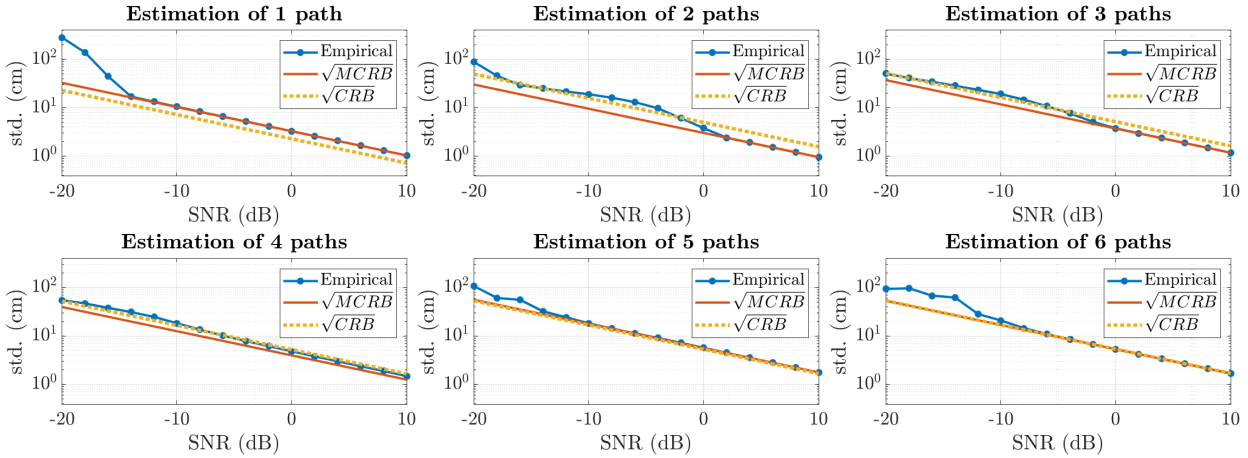

FIGURE 10. Standard deviation of the estimated delay of the first arriving path for the $L = 6$ paths channel impulse response shown in fig. 7 as a function of SNR. The empirical results are obtained using the steepest descent method over 2000 realizations (blue), the MCRB is computed with (49), (50), and the CRB with (14), (20) and (21). Each subplot corresponds to a different number of jointly estimated paths $\hat{L}$.

crossing point moves to larger path separations because the variance of the 2-path MLE (green curve) increases. As a result, the paths must be even further apart before the more complex model provides a performance improvement.

IX. NUMERICAL RESULTS AND VALIDATION

In this section we compare the bound on the MSE of the time-delay estimator for the first path with the empirical MSE obtained via Montecarlo simulation. The channel impulse response is modeled with six paths with fixed time-delays and gains (see Fig. 7). To create a challenging scenario for estimating the first arriving path, a strong close-in multipath is placed at a distance $c\tau_{21} = 2$ m, which is comparable to the width of the signal ACF main peak of $c/B = 1.87$ m. Additionally, four weaker paths are placed starting from a distance of 8 m, with 4-meter equispacing. For each simulation run, a new noise realization is generated, while the delay, gain and relative phase of the paths remain constant. The SNR is defined with respect to the first path as $|x_1|^2/\sigma_n^2$.

The MSE bound is evaluated using (60). The bias and the pseudotrue parameter $\boldsymbol{\theta}_0$ are obtained by solving the minimization problem in (44) with the Steepest Descent algorithm. The empirical results are obtained by estimating the time-delay of the first path over 2000 realizations. Time-delay estimation is done by solving (9) using the Steepest Descent algorithm.

Figure 8 shows that the bias of the first arriving path decreases as more paths are considered in the estimation model. In contrast, the CRB exhibits the opposite trend, since jointly estimating additional paths increases the estimation variance, also for the first arriving path. Unlike the CRB, the MCRB can decrease when an extra path is added to the model

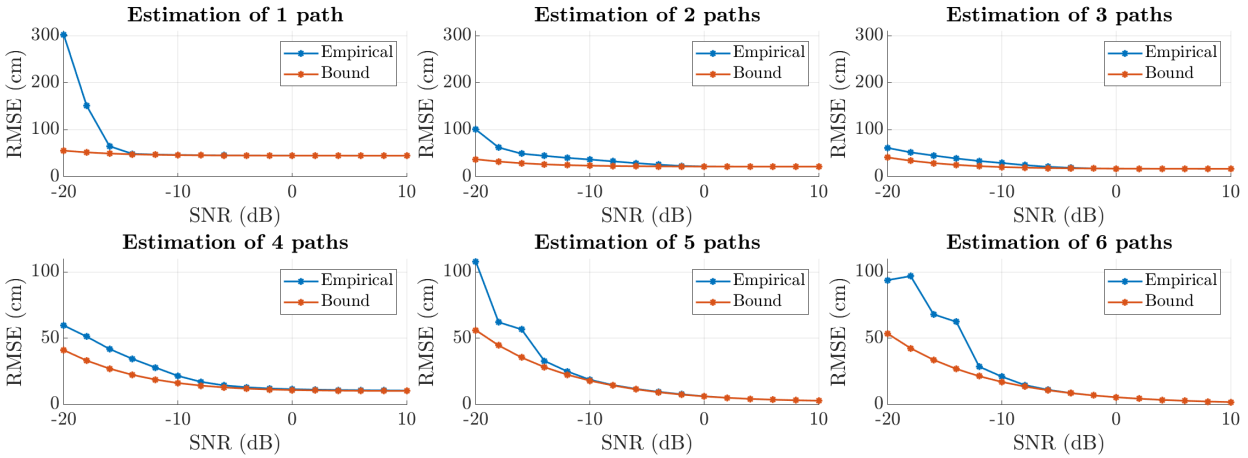

FIGURE 11. RMSE of the estimated delay of the first arriving path for the $L = 6$ paths channel impulse response shown in fig. 7 as a function of SNR. The empirical results are obtained using the steepest descent method over 2000 realizations (blue) and the bound is computed with the bias-variance decomposition in (60) (red), based on the MCRB. Each subplot corresponds to a different number of jointly estimated paths $\hat{L}$.

depending on the relative delay, gain and carrier phase of the unconsidered multipath components.

Figures 9, 10, and 11 compare the theoretical bounds with the empirical results for the bias, standard deviation, and RMSE. As shown in Fig. 9, the empirical mean error (blue curve) aligns closely with the theoretical bias (red line) at mid-to-high SNR (above 0 dB). This agreement confirms that the time-delay estimator converges to the pseudotrue parameter for large SNR (32). At low SNR, the discrepancy between the empirical mean and the theoretical bias increases, primarily due to sidelobe acquisitions (thresholding effect).

Figure 10 compares the empirical standard deviation of the estimation errors against the square roots of the MCRB and CRB. The MCRB is smaller than the empirical standard deviation for all SNR. Moreover, the empirical standard deviation converges to the MCRB for mid-to-high SNR. This agrees with the fact that the variance of the estimator converges to the MCRB for large SNR (32). At low SNR, the discrepancy between the MCRB and the empirical standard deviation arises because the MCRB is computed at the pseudotrue parameter, and for low SNR the mean empirical error does not match the pseudotrue parameter due to the thresholding effect, as shown in fig. 9. Contrary to the MCRB, the CRB is not a reliable lower-bound. For instance, when two paths are estimated, the square root of the CRB exceeds the empirical standard deviation for SNR above 0 dB, yet falls bellow the empirical standard deviation in the -15 dB to 0 dB range (see fig. 10).

Finally, Fig. 11 confirms that the empirical RMSE is always lower-bounded by the theoretical RMSE based on the MCRB, and converges to this bound at mid-to-high SNR. This validates the theoretical MSE bound derived in this work.

Figure 12 shows the ranging RMSE bound (left) and the empirical RMSE (right) by MLE estimators that assume $\hat{L} = 1, \ldots, 6$ paths, in an $L = 6$ paths channel (fig. 7), as a function of SNR. The RMSE bound and the empirical RMSE correspond to the red and blue curves in fig. 11, respectively. At high SNR, the bound and the empirical results match. At low SNR, the empirical RMSE exceeds the bound, which does not account for the thresholding effect. Additionally, at -20 dB of SNR, the bound suggests that the MLE achieves the best performance for $\hat{L} = 2, 3, 4$, whereas the empirical results indicate that the MLE with $\hat{L} = 3$ and 4 yield the best performance. This discrepancy arises because the bound does not capture the impact of the thresholding effect, limiting its applicability for low SNR.

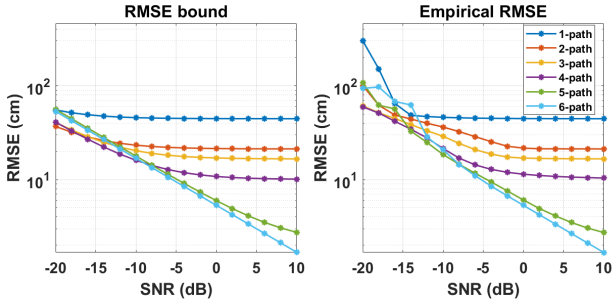

FIGURE 12. RMSE of estimated delay of the first arriving path for $\hat{L} = 1, \ldots, 6$ paths for the $L = 6$ paths channel impulse response shown in Fig. 7 as a function of SNR. The bound is computed using the bias-variance decomposition in (60) (left) and empirical results are obtained using the steepest descent method over 2000 realizations (right). RMSE bound and empirical RMSE correspond to the red and blue curves in Fig. 11, respectively.

At high SNR, adding more paths to the estimation model substantially reduces the bias associated with each path without a corresponding increase in variance. Therefore, the largest performance gain obtained by adding more paths in the estimation model occurs at high SNR.

The six-path MLE is unbiased, as its model-order matches the number of paths in the channel, and in this case, achieves the best empirical performance over almost the entire SNR regime. However, the six-path MLE is the most computationally expensive. As a trade-off between RMSE and computational efficiency, one may choose an estimator with fewer paths, while still meeting a target RMSE. For example, if the ranging RMSE requirement is 20 cm at 0 dB of SNR, the MLE that accounts for $\hat{L} = 3, 4, 5$ paths is sufficient in this scenario. The provided RMSE bound can be used to guide the selection of the number of paths in the estimation model for different deterministic channels, particularly in the high SNR regime.

X. CONCLUSION

The fundamental challenge of time-delay estimation for ranging in multipath channels is that only the first path is of interest, yet ignoring subsequent paths may severely degrade estimator performance. In this misspecified scenario, estimation bias may occur, and the variance of the estimator may no longer be the one expected by the CRB.

In this paper, we derived bounds on the variance using the MCRB of a misspecified estimator that accounts for fewer propagation paths than actually present. For two-path channels, we have demonstrated a clear distinction between the behaviour of bias and variance: while the bias is bounded by the classical multipath error envelope, the variance can be upper- and lower-bounded by constructive and destructive multipath components but not strictly for all path separations. We have shown that the MSE can be bounded through the bias-variance decomposition, with the variance given by the MCRB. This bound tightly matches the MSE of maximum-likelihood estimators at mid-to-high SNR values, where sidelobe acquisitions rarely occur.

Although we derived the bounds using an OFDM signal model, the underlying framework relies solely on bandlimited channel frequency response measurements. Therefore, the framework is generally applicable to any system that estimates the channel frequency response over a finite bandwidth.

We adopted a deterministic channel model, with fixed path delays and gains. Using a deterministic parametrization of the gains, rather than a Bayesian one, enables a clear assessment of the impact of multipath components with different relative carrier phases. Moreover, modelling the paths with deterministic delays allows us to analyse how estimation variance behaves as a function of the path separation.

This work focuses solely on the impact of multipath in time-delay estimation, while assuming that the carrier frequency offset and the Doppler frequency shift are compensated prior to performing TDE. The impact of multipath channels for the not perfectly synchronized OFDM receiver is left for future work. The examples provided in this paper considered LOS scenarios in which the first arriving path is always the strongest, though for NLOS conditions the same expressions for the bias and the MCRB can be applied.

The presented performance bounds on the time-delay estimator of the first path help to understand the impact of unmodelled multipath on the bias and the variance, and are crucial for designing ranging signals for challenging scenarios. Moreover, these performance bounds can be used as a criterion to determine the optimum number of paths to consider in the time-delay estimation model. As a general rule, adding more paths in the estimation model decreases the bias at the expense of increasing the estimation variance.

APPENDIX A
GRADIENT AND JACOBIAN MATRIX

The gradient vector of a scalar function $q(\boldsymbol{\theta})$ with parameters $\boldsymbol{\theta} = [\theta_1, \theta_2, \cdots, \theta_M]^T$, is a column vector with M entries

$$\frac{\partial q(\boldsymbol{\theta})}{\partial \boldsymbol{\theta}} \triangleq \left[\frac{\partial q(\boldsymbol{\theta})}{\partial \theta_1}, \frac{\partial q(\boldsymbol{\theta})}{\partial \theta_2}, \ldots, \frac{\partial q(\boldsymbol{\theta})}{\partial \theta_M}\right]^T. \tag{61}$$

Let $\boldsymbol{q}(\boldsymbol{\theta})$ be a multivariate function

$$\boldsymbol{q}(\boldsymbol{\theta}) \triangleq [q_1(\boldsymbol{\theta}), q_2(\boldsymbol{\theta}), \cdots, q_m(\boldsymbol{\theta})]^T, \tag{62}$$

then, the Jacobian matrix of $\boldsymbol{q}(\boldsymbol{\theta})$ is expressed in terms of its column vectors as

$$\frac{\partial \boldsymbol{q}(\boldsymbol{\theta})}{\partial \boldsymbol{\theta}^T} \triangleq \left[\frac{\partial \boldsymbol{q}(\boldsymbol{\theta})}{\partial \theta_1} \; \frac{\partial \boldsymbol{q}(\boldsymbol{\theta})}{\partial \theta_2} \; \cdots \; \frac{\partial \boldsymbol{q}(\boldsymbol{\theta})}{\partial \theta_M}\right], \tag{63}$$

and in expanded form, it is

$$\frac{\partial \boldsymbol{q}(\boldsymbol{\theta})}{\partial \boldsymbol{\theta}^T} \triangleq \begin{bmatrix} \frac{\partial q_1(\boldsymbol{\theta})}{\partial \theta_1} & \frac{\partial q_1(\boldsymbol{\theta})}{\partial \theta_2} & \cdots & \frac{\partial q_1(\boldsymbol{\theta})}{\partial \theta_M} \\ \frac{\partial q_2(\boldsymbol{\theta})}{\partial \theta_1} & \frac{\partial q_2(\boldsymbol{\theta})}{\partial \theta_2} & \cdots & \frac{\partial q_2(\boldsymbol{\theta})}{\partial \theta_M} \\ \vdots & \vdots & & \vdots \\ \frac{\partial q_m(\boldsymbol{\theta})}{\partial \theta_1} & \frac{\partial q_m(\boldsymbol{\theta})}{\partial \theta_2} & \cdots & \frac{\partial q_m(\boldsymbol{\theta})}{\partial \theta_M} \end{bmatrix}, \tag{64}$$

where $\frac{\partial \boldsymbol{q}(\boldsymbol{\theta})}{\partial \theta_i} \in \mathbb{R}^{m\times 1}$, and $\frac{\partial \boldsymbol{q}(\boldsymbol{\theta})}{\partial \boldsymbol{\theta}^T} \in \mathbb{R}^{m\times M}$.

Each element of the Hessian matrix of a scalar function $q(\boldsymbol{\theta})$ is defined as

$$\left[\frac{\partial^2 q(\boldsymbol{\theta})}{\partial \boldsymbol{\theta} \partial \boldsymbol{\theta}^T}\right]_{i,k} = \frac{\partial^2 q(\boldsymbol{\theta})}{\partial \theta_i \partial \theta_k}, \tag{65}$$

where the indices i and k range from 1 to M.

APPENDIX B
ENTRIES OF FIM AND DOUBLE DERIVATIVES

The partial derivatives of $\boldsymbol{\mu}(\boldsymbol{\theta})$ in (6) with respect to τ_i and x_i are given by:

$$\begin{aligned} \frac{\partial \boldsymbol{\mu}(\boldsymbol{\theta})}{\partial \tau_i} &= -j2\pi x_i \mathbf{f} \odot \mathbf{a}(\tau_i), \\ \frac{\partial \boldsymbol{\mu}(\boldsymbol{\theta})}{\partial \Re\{x_i\}} &= \mathbf{a}(\tau_i), \quad \frac{\partial \boldsymbol{\mu}(\boldsymbol{\theta})}{\partial \Im\{x_i\}} = j\mathbf{a}(\tau_i). \end{aligned} \tag{66}$$

The elements of the FIM follow as:

$$\frac{\partial \boldsymbol{\mu}^H(\boldsymbol{\theta})}{\partial \tau_i} \frac{\partial \boldsymbol{\mu}(\boldsymbol{\theta})}{\partial \tau_i} = 4\pi^2 |x_i|^2 \mathbf{f}^T \mathbf{f},$$

$$\begin{aligned}
\frac{\partial \boldsymbol{\mu}^H(\boldsymbol{\theta})}{\partial \tau_i}\frac{\partial \boldsymbol{\mu}(\boldsymbol{\theta})}{\partial \tau_k} &= 4\pi^2 x_i^H x_k \mathbf{a}^T(\tau_k-\tau_i)(\mathbf{f}\odot\mathbf{f}),\\
\frac{\partial \boldsymbol{\mu}^H(\boldsymbol{\theta})}{\partial \Re\{x_i\}}\frac{\partial \boldsymbol{\mu}(\boldsymbol{\theta})}{\partial \Re\{x_i\}} &= \frac{\partial \boldsymbol{\mu}^H(\boldsymbol{\theta})}{\partial \Im\{x_i\}}\frac{\partial \boldsymbol{\mu}(\boldsymbol{\theta})}{\partial \Im\{x_i\}} = N_s,\\
\frac{\partial \boldsymbol{\mu}^H(\boldsymbol{\theta})}{\partial \Re\{x_i\}}\frac{\partial \boldsymbol{\mu}(\boldsymbol{\theta})}{\partial \Re\{x_k\}} &= \mathbf{a}^T(\tau_k-\tau_i)\mathbf{1}_{N_s},
\end{aligned} \tag{67}$$

and

$$\begin{aligned}
\frac{\partial \boldsymbol{\mu}^H(\boldsymbol{\theta})}{\partial \tau_i}\frac{\partial \boldsymbol{\mu}(\boldsymbol{\theta})}{\partial \Re\{x_k\}} &= j2\pi x_i^H \mathbf{f}^T\mathbf{a}(\tau_k-\tau_i),\\
\frac{\partial \boldsymbol{\mu}^H(\boldsymbol{\theta})}{\partial \tau_i}\frac{\partial \boldsymbol{\mu}(\boldsymbol{\theta})}{\partial \Im\{x_k\}} &= -2\pi x_i^H \mathbf{f}^T\mathbf{a}(\tau_k-\tau_i),\\
\frac{\partial \boldsymbol{\mu}^H(\boldsymbol{\theta})}{\partial \Re\{x_i\}}\frac{\partial \boldsymbol{\mu}(\boldsymbol{\theta})}{\partial \Im\{x_k\}} &= j\mathbf{a}^T(\tau_k-\tau_i)\mathbf{1}_{N_s},\\
\frac{\partial \boldsymbol{\mu}^H(\boldsymbol{\theta})}{\partial \Im\{x_i\}}\frac{\partial \boldsymbol{\mu}(\boldsymbol{\theta})}{\partial \Re\{x_k\}} &= -j\mathbf{a}^T(\tau_k-\tau_i)\mathbf{1}_{N_s},
\end{aligned} \tag{68}$$

where $\mathbf{1}_{N_s}$ is the all-ones column vector with N_s entries.

The elements of the second derivatives are given by

$$\begin{aligned}
\frac{\partial^2 \boldsymbol{\mu}^H(\boldsymbol{\theta})}{\partial \tau_i \partial \tau_i} &= -4\pi^2 x_i^H(\mathbf{f}\odot\mathbf{f}\odot\mathbf{a}(-\tau_i))^T,\\
\frac{\partial^2 \boldsymbol{\mu}^H(\boldsymbol{\theta})}{\partial \tau_i \partial \tau_k} &= \frac{\partial^2 \boldsymbol{\mu}^H(\boldsymbol{\theta})}{\partial \tau_i \partial \Re\{x_k\}} = \mathbf{0}_{N_s}^T, \quad \text{for } i \neq k,\\
\frac{\partial^2 \boldsymbol{\mu}^H(\boldsymbol{\theta})}{\partial \tau_i \partial \Re\{x_i\}} &= j\,2\pi(\mathbf{f}\odot\mathbf{a}(-\tau_i))^T,\\
\frac{\partial^2 \boldsymbol{\mu}^H(\boldsymbol{\theta})}{\partial \tau_i \partial \Im\{x_i\}} &= 2\pi(\mathbf{f}\odot\mathbf{a}(-\tau_i))^T,\\
\frac{\partial^2 \boldsymbol{\mu}^H(\boldsymbol{\theta})}{\partial \tau_i \partial \Im\{x_k\}} &= \mathbf{0}_{N_s}^T, \quad \text{for } i \neq k,\\
\frac{\partial^2 \boldsymbol{\mu}^H(\boldsymbol{\theta})}{\partial \Re\{x_i\} \partial \Re\{x_k\}} &= \frac{\partial^2 \boldsymbol{\mu}^H(\boldsymbol{\theta})}{\partial \Im\{x_i\} \partial \Im\{x_k\}} = \mathbf{0}_{N_s}^T, \quad \forall\, i,k,\\
\frac{\partial^2 \boldsymbol{\mu}^H(\boldsymbol{\theta})}{\partial \Re\{x_i\} \partial \Im\{x_k\}} &= \mathbf{0}_{N_s}^T, \quad \forall\, i,k,
\end{aligned} \tag{69}$$

where $\mathbf{0}_{N_s}^T$ is a row vector of zeros with N_s entries.

APPENDIX C
DERIVATIVES OF ACF AND CROSS-CORRELATION FUNCTION

The first- and second-order derivatives of the ACF in (19) are obtained as:

$$\begin{aligned}
R_s'(\tau) &= \frac{\delta R_s(\tau)}{\delta \tau} = -j2\pi \mathbf{f}^T\mathbf{a}(\tau),\\
R_s''(\tau) &= \frac{\delta^2 R_s(\tau)}{\delta \tau^2} = -4\pi^2(\mathbf{f}\odot\mathbf{f})^T\odot\mathbf{a}(\tau),
\end{aligned} \tag{70}$$

which, when evaluated at $\tau = 0$ reduces to

$$R_s''(0) = \left.\frac{\delta^2 R_s(\tau)}{\delta \tau^2}\right|_{\tau=0} = -4\pi^2 \mathbf{f}^T\mathbf{f}. \tag{71}$$

Likewise, the first- and second-order derivatives of the cross-correlation function in (19) are given by:

$$\begin{aligned}
R_{\boldsymbol{\mu},\mathbf{d}}'(\tau) &= -j|x_1|^2 2\pi \mathbf{f}^T\mathbf{a}(\tau_1-\tau) - jx_1^H x_2 2\pi \mathbf{f}^T\mathbf{a}(\tau_2-\tau),\\
R_{\boldsymbol{\mu},\mathbf{d}}''(\tau) &= -|x_1|^2 4\pi^2(\mathbf{f}\odot\mathbf{f})\mathbf{a}(\tau_1-\tau)\\
&\quad - x_1^H x_2 4\pi^2(\mathbf{f}\odot\mathbf{f})\mathbf{a}(\tau_2-\tau)\\
&= -4\pi^2(x_1^H x_1\mathbf{a}(\tau_1-\tau)\\
&\quad + x_1^H x_2\mathbf{a}(\tau_2-\tau))^T(\mathbf{f}\odot\mathbf{f}).
\end{aligned} \tag{72}$$

REFERENCES

[1] K. Shamaei and Z. M. Kassas, "Receiver design and time of arrival estimation for opportunistic localization with 5G signals," *IEEE Trans. Wireless Commun.*, vol. 20, no. 7, pp. 4716–4731, Jul. 2021.
[2] J. A. del Peral-Rosado, J. A. López-Salcedo, F. Zanier, and G. Seco-Granados, "Position accuracy of joint time-delay and channel estimators in LTE networks," *IEEE Access*, vol. 6, pp. 25185–25199, 2018.
[3] L. A. Navarro, C. C. J. M. Tiberius, and G. J. M. Janssen, "Maximum likelihood time-delay estimation in multipath channels with two-and three-paths models using OFDM," in *Proc. IEEE/ION Position, Location Navigat. Symp. (PLANS)*, Apr. 2025, pp. 968–979.
[4] P. Stoica and Y. Selen, "Model-order selection: A review of information criterion rules," *IEEE Signal Process. Mag.*, vol. 21, no. 4, pp. 36–47, Apr. 2004.
[5] C. D. Richmond and L. L. Horowitz, "Parameter bounds on estimation accuracy under model misspecification," *IEEE Trans. Signal Process.*, vol. 63, no. 9, pp. 2263–2278, May 2015.
[6] S. Fortunati, F. Gini, M. S. Greco, and C. D. Richmond, "Performance bounds for parameter estimation under misspecified models: Fundamental findings and applications," *IEEE Signal Process. Mag.*, vol. 34, no. 6, pp. 142–157, Nov. 2017.
[7] C. Lubeigt, L. Ortega, J. Vilà-Valls, and E. Chaumette, "Untangling first and second order statistics contributions in multipath scenarios," *Signal Process.*, vol. 205, Apr. 2023, Art. no. 108868.
[8] R. Duprat, E. Ghizzo, P. Thevenon, L. Ortega, S. Roche, M. Bouilhac, and F.-X. Marmet, "Performance evaluation of GNSS meta-signals under multipath environment," in *Proc. ION GNSS+, Int. Tech. Meeting Satell. Division Inst. Navigat.*, Sep. 2025, pp. 878–898. [Online]. Available: https://www.ion.org/publications/abstract.cfm?articleID=20404
[9] A. N. D'Andrea, U. Mengali, and R. Reggiannini, "The modified Cramer–Rao bound and its application to synchronization problems," *IEEE Trans. Commun.*, vol. 42, no. 234, pp. 1391–1399, Feb. 1994.
[10] Y. Wang, G. Leus, and A.-J. van der Veen, "Cramér–Rao bound for range estimation," in *Proc. IEEE Int. Conf. Acoust., Speech Signal Process.*, Apr. 2009, pp. 3301–3304.
[11] S. M. Kay, *Fundamentals of Statistical Signal Processing: Estimation Theory*, 1st ed., Upper Saddle River, NJ, USA: Prentice-Hall, 1993.
[12] E. W. Barankin, "Locally best unbiased estimates," *Ann. Math. Statist.*, vol. 20, no. 4, pp. 477–501, Dec. 1949.
[13] H. Dun, C. C. J. M. Tiberius, C. E. V. Diouf, and G. J. M. Janssen, "Design of sparse multiband signal for precise positioning with joint low-complexity time delay and carrier phase estimation," *IEEE Trans. Veh. Technol.*, vol. 70, no. 4, pp. 3552–3567, Apr. 2021.
[14] T. Wang, Y. Shen, S. Mazuelas, H. Shin, and M. Z. Win, "On OFDM ranging accuracy in multipath channels," *IEEE Syst. J.*, vol. 8, no. 1, pp. 104–114, Mar. 2014.
[15] H. L. Van Trees and K. L. Bell, *Bayesian Bounds for Parameter Estimation and Nonlinear Filtering/Tracking*. Piscataway, NJ, USA: IEEE Press, 2007.
[16] K. L. Bell, Y. Steinberg, Y. Ephraim, and H. L. Van Trees, "Extended ziv-zakai lower bound for vector parameter estimation," *IEEE Trans. Inf. Theory*, vol. 43, no. 2, pp. 624–637, Mar. 1997.
[17] J. Ziv and M. Zakai, "Some lower bounds on signal parameter estimation," *IEEE Trans. Inf. Theory*, vol. IT-15, no. 3, pp. 386–391, May 1969.
[18] A. Graff and T. E. Humphreys, "Purposeful co-design of OFDM signals for ranging and communications," *EURASIP J. Adv. Signal Process.*, vol. 2024, no. 1, Jan. 2024, Art. no. 20.
[19] H. L. V. Trees, K. L. Bell, and Z. Tian, *Detection, Estimation, and Modulation Theory, Part I: Detection, Estimation, and Filtering Theory*, 2nd ed., Hoboken, NJ, USA: Wiley, May 2013.

[20] A. Mallat, S. Gezici, D. Dardari, C. Craeye, and L. Vandendorpe, "Statistics of the MLE and approximate upper and lower bounds—Part I: Application to TOA estimation," *IEEE Trans. Signal Process.*, vol. 62, no. 21, pp. 5663–5676, Nov. 2014.
[21] A. G. Amigó, P. Closas, A. Mallat, and L. Vandendorpe, "Ziv-zakai lower bound for UWB based TOA estimation with unknown interference," in *Proc. IEEE Int. Conf. Acoust., Speech Signal Process. (ICASSP)*, May 2014, pp. 6504–6508.
[22] P. J. Huber, "The behavior of maximum likelihood estimates under nonstandard conditions," in *Proc. 5th Berkeley Symp. Math. Statist. Probab.*, California, 1967, pp. 221–234.
[23] H. Akaike, "A new look at the statistical model identification," *IEEE Trans. Autom. Control*, vol. AC-19, no. 6, pp. 716–723, Dec. 1974.
[24] H. White, "Maximum likelihood estimation of misspecified models," *Econometrica*, vol. 50, no. 1, pp. 1–25, Jan. 1982.
[25] M. Levy-Israel, I. Bilik, and J. Tabrikian, "MCRB on DOA estimation for automotive MIMO radar in the presence of multipath," *IEEE Trans. Aerosp. Electron. Syst.*, vol. 59, no. 5, pp. 4831–4843, May 2023.
[26] H. Chen, S. R. Aghdam, M. F. Keskin, Y. Wu, S. Lindberg, A. Wolfgang, U. Gustavsson, T. Eriksson, and H. Wymeersch, "MCRB-based performance analysis of 6G localization under hardware impairments," in *Proc. IEEE Int. Conf. Commun. Workshops (ICC Workshops)*, May 2022, pp. 115–120.
[27] P. Zheng, H. Chen, T. Ballal, H. Wymeersch, and T. Y. Al-Naffouri, "Misspecified Cramér–Rao bound of RIS-aided localization under geometry mismatch," in *Proc. IEEE Int. Conf. Acoust., Speech Signal Process. (ICASSP)*, Jun. 2023, pp. 1–5.
[28] N. Harel and T. Routtenberg, "Non-Bayesian post-model-selection estimation as estimation under model misspecification," *IEEE Trans. Signal Process.*, vol. 72, pp. 3641–3657, 2024.
[29] Y. G. Li and G. L. Stüber, *Orthogonal Frequency Division Multiplexing for Wireless Communications*. Cham, Switzerland: Springer, 2006.
[30] M. Morelli and U. Mengali, "A comparison of pilot-aided channel estimation methods for OFDM systems," *IEEE Trans. Signal Process.*, vol. 49, no. 12, pp. 3065–3073, Dec. 2001.
[31] G. H. Golub and V. Pereyra, "The differentiation of pseudo-inverses and nonlinear least squares problems whose variables separate," *SIAM J. Numer. Anal.*, vol. 10, no. 2, pp. 413–432, Apr. 1973.
[32] J. Yan, C. C. J. M. Tiberius, G. J. M. Janssen, P. J. G. Teunissen, and G. Bellusci, "Review of range-based positioning algorithms," *IEEE Aerosp. Electron. Syst. Mag.*, vol. 28, no. 8, pp. 2–27, Aug. 2013.
[33] A. Renaux, P. Forster, E. Chaumette, and P. Larzabal, "On the high-SNR conditional maximum-likelihood estimator full statistical characterization," *IEEE Trans. Signal Process.*, vol. 54, no. 12, pp. 4840–4843, Dec. 2006.
[34] F. A. M. Meurer, "Signals and modulation," in *Springer Handbook of Global Navigation Satellite Systems*, P. Teunissen and O. Montenbruck, Eds., New York, NY, USA: Springer, 2017, ch. 4.
[35] L. Ortega, C. Lubeigt, J. Vilà-Valls, and E. Chaumette, "On GNSS synchronization performance degradation under interference scenarios: Bias and misspecified Cramér–Rao bounds," *Navigation*, vol. 70, no. 4, 2023.
[36] A. P. Dempster, N. M. Laird, and D. B. Rubin, "Maximum likelihood from incomplete data via the EM algorithm," *J. Roy. Stat. Soc. Ser. B, Stat. Methodol.*, vol. 39, no. 1, pp. 1–38, Sep. 1977.
[37] I. Ziskind and M. Wax, "Maximum likelihood localization of multiple sources by alternating projection," *IEEE Trans. Acoust., Speech, Signal Process.*, vol. ASSP-36, no. 10, pp. 1553–1560, Oct. 1988.
[38] J. A. Fessler and A. O. Hero, "Space-alternating generalized expectation-maximization algorithm," *IEEE Trans. Signal Process.*, vol. 42, no. 10, pp. 2664–2677, Oct. 1994.
[39] M. S. Braasch, "Multipath," in *Springer Handbook of Global Navigation Satellite Systems*, P. Teunissen and O. Montenbruck, Eds., New York, NY, USA: Springer, 2017, ch. 1.
[40] J. A. Del Peral-Rosado, J. A. López-Salcedo, G. Seco-Granados, F. Zanier, and M. Crisci, "Joint maximum likelihood time-delay estimation for LTE positioning in multipath channels," *EURASIP J. Adv. Signal Process.*, vol. 2014, no. 1, p. 33, Dec. 2014.

LUCAS ALVAREZ NAVARRO received the M.Sc. degree in telecommunications engineering from the Universitat Autónoma de Barcelona (UAB), in 2022. He is currently pursuing the Ph.D. degree with the Department of Geoscience and Remote Sensing, Delft University of Technology, The Netherlands. After his M.Sc. degree, he joined Qascom S.r.l and later GMV as a Radio Navigation Engineer. His interests include navigation and statistical signal processing for GNSS and terrestrial radio positioning.

CHRISTIAN C. J. M. TIBERIUS received the Ph.D. degree from Delft University of Technology, in 1998, with a focus on the subject of recursive data processing for kinematic GPS surveying. He is currently an Associate Professor with the Geoscience and Remote Sensing (GRS) Department, Delft University of Technology. His research interests include navigation, with GNSS and terrestrial radio positioning, primarily for automotive applications.

GERARD J. M. JANSSEN received the Ph.D. degree from Delft University of Technology, Delft, The Netherlands, in 1998. He is currently an Associate Professor with the Signal Processing Systems Group, Delft University of Technology. His research interests include wireless communication, particularly narrowband multiuser detection, digital modulation techniques, channel modeling, diversity techniques, and ultra-wideband communication and positioning.